Published in "Galactic and Extragalactic Radio Astronomy", 1988, 2nd edition, eds. G.L. Verschuur and K.I. Kellerman.

12. EXTRAGALACTIC NEUTRAL HYDROGEN

Riccardo Giovanelli and Martha P. Haynes

Table of Contents

12.1. INTRODUCTION

The 21-cm hyperfine transition of neutral hydrogen was first detected in the Milky Way in 1951 by Ewen and Purcell. Two years later (Kerr and Hindman 1953), the HI emission of the Magellanic Clouds was observed from Australia. Largely as a result of the pioneering efforts of M.S. Roberts, by the time of his comprehensive review (Roberts 1975; the reader is referred to this source for the early development of the field), HI in about 140 extragalactic objects had been detected. Since then, mostly with the Green Bank 91-m, the Nançay, the Effelsberg, and more recently the Arecibo telescopes, the line has been observed in emission in thousands of galaxies, to distances 10^4 times greater than that of the Magellanic Clouds, and in absorption out to redshifts greater than 2. For the first twenty years, single-dish telescopes provided the vast majority of the HI data. By the mid-seventies, the techniques of spectral line aperture synthesis, developed especially at Cambridge, Green Bank, and Owens Valley, bloomed in full maturity at Westerbork and more recently at the VLA. The contributions of single-dish instruments have, however, remained important, especially for survey-oriented projects that require high sensitivity observations of many noncontiguous regions of sky, and for pure detection experiments.

12.1.1. The Role of Neutral Hydrogen in Galaxies

Neutral-hydrogen concentrations, or clouds, provide the starting point for the collapse of matter into stars. Abundant HI in a galaxy indicates potentially active star formation processes, while lack of HI is a guarantee of a barren galaxy and an ineluctably aging stellar population. Thus, from an evolutionary viewpoint, the role of HI is of primary importance. Dynamically, that is, in terms of the fractional contribution to the mass, the perspective is different and, as discussed in detail in Section 12.5, quite dependent on morphological type. The Milky Way provides a reference point. Our Galaxy is an intermediate- to late-type spiral, perhaps an Sbc. The optical surface brightness of the disk decreases exponentially with distance from the center, with one-half of the spatially integrated luminosity falling within an effective radius of 4 or 5 kpc; the luminosity of the entire disk is about $1.1 \times 10^{10}\ L_\odot$, twice that of the nuclear bulge. Although ionized gas is found in the halo, the bulk of the interstellar gas is in the disk; similarly to the light, but with the exception of the very central regions, the total hydrogen gas (HI + H II + H_2) component mimics an exponential disk, with an effective radius close to that of the optical emission. While molecular hydrogen is the dominant constituent of the interstellar medium

within the solar circle, atomic hydrogen predominates towards the periphery of the disk. In fact, HI extends farther out than any other galactic disk tracer. By mass, the atomic hydrogen resides mostly in diffuse clouds and in the envelopes surrounding molecular clouds. The thickness of the HI disk is nearly constant within the inner 10 to 12 kpc, the averaged density falling to half its peak value at the plane at about 150 to 200 pc from it. A density cross section perpendicular to the plane does, however, show weak, broad wings, associated with a warmer, less clumped HI component of the interstellar medium, more than twice as thick as the main disk component. The total amount of interstellar hydrogen in the inner 16 kpc of the Galaxy is about 6×10^9 $M_\odot$, with roughly half in molecular and half in atomic form. While the atomic gas extends well outside that radius, the contribution of the gas (as well as that of all luminous matter) to the total mass decreases sharply with distance, and probably the total gaseous mass of the Galaxy does not exceed 10^{10} $M_\odot$. As the luminous mass fades rapidly in the outer regions of the Galaxy, the dynamical mass traced by the system of globular clusters and by the dwarf spheroidal satellites of the Milky Way continues to grow almost linearly with distance from the center. Within 16 kpc from the center, this mass is 1.5×10^{11} $M_\odot$, rising to about 10^{12} $M_\odot$ inside 100 kpc. Atomic hydrogen thus represents less than 10% of the total mass within the easily discernible stellar disk, and about 1% of the total mass out to 100 kpc. Its importance relative to other constituents grows for galaxies of later morphological type than our own; within the region mapped by the HI in some extremely optically-faint blue galaxies, HI can be the principal constituent of the visible mass. By contrast, very early spiral and lenticular galaxies frequently have less than 0.01% of their mass in the form of neutral hydrogen gas, ellipticals sometimes even less.

12.1.2. The Information in the 21-cm Line

Although in most cases HI is just a tracer component of the makeup of a galaxy, it constitutes an important tool in the study of the structure and dynamics of galaxy evolution. Notable reasons for the popularity of the line as such a tool are the ease of detection and the relative reliability of the column densities and other physical parameters inferred from the line profiles.

The 21-cm line results from a magnetic dipole transition between the two levels that characterize the ground state of the hydrogen atom. Depending on whether the electronic and nuclear spin vectors are parallel or antiparallel, a slightly higher (triplet) or lower (singlet) hyperfine level is obtained. The statistical equilibrium between the populations of the singlet and triplet levels can be expressed by means of the Boltzmann equation, in which the effective temperature that regulates the relative populations is referred to as the "spin temperature," T_s. Several processes contribute to T_s; the most important, as originally described by Field (1959), are: (i) absorption of and emission stimulated by photons of an existing radiation field; (ii) collisions of H atoms with other particles, especially with other H atoms and with electrons; (iii) "pumping" by Lyman α photons. As an example of the last process, a H atom in the singlet state of $n = 1$ can be excited to the $n = 2$ state by a Lyman α photon; subsequent deexcitation to the $n = l$ level will leave the H atom in the triplet level in a fraction of the cases. Spontaneous transitions from the triplet to the singlet level occur with a transition probability $A_{10} = 2.868 \times 10^{-15}$ s^{-1}; in most cases of interest, however, a H atom will not be left alone for as long as eleven million years, and so T_s is largely determined by the above-mentioned extrinsic influences.

A cloud of optical depth τ and spin temperature T_s, bathed in a radiation field of temperature T_r, will yield a brightness temperature

$$T_b(v) = T_r e^{-\tau(v)} + T_s[1 - e^{-\tau(v)}] \qquad (12.1)$$

where the optical depth $\tau(v)$ varies with velocity v across the line profile. The optical depth $\tau(v)$ can be expressed as the ratio of the HI column density to the spin temperature (see Spitzer 1978). If one assumes that the gas is optically thin (i.e., $\tau << 1$), the column density of HI can then be obtained as

$$N_H = 1.82 \times 10^{13} \int \left(\frac{T_s}{T_s - T_r} \right) T_{bl}(v) dv \qquad \text{atoms cm}^{-2} \qquad (12.2)$$

where $T_{bl}(v)$ is the brightness temperature of the line profile at velocity v, in cm s^{-1}, above the continuum or baseline level, and the integral is over the line profile. Over most of the HI mass of a galactic disk, collisions determine the population of the two $n = 1$ hyperfine levels, and T_s closely approaches the kinetic temperature of the gas. Since this is usually much larger than T_r the term in square brackets in Equation (12.2) is about unity. In the outer regions of the disks, and in envelopes of tidal debris after galaxy-galaxy interactions, where gas densities are low and collisions rare, T_s will be regulated by the radiation field at 21 cm and at 1216 Å (Lyman α). The former will be dominated by the cosmic background radiation at 2.7 K; in the absence of a sufficient ionizing flux, the term [T_s / (T_s) - T_r)] could be significantly larger than 1, and the determination of N_H would require a knowledge of T_s, which is difficult to obtain. Watson and Deguchi (1984) have shown, however, that the Lyman a flux in intergalactic space may be large enough that Lyman α pumping regulates the populations of the hyperfine levels and tends to push T_s to values well above 2.7 K, thus suggesting that even in very-low-density clouds outside of disks, [T_s / (T_s) - T_r)] remains close to 1. A simple integral across the line then will give a close estimate of the atomic hydrogen column density. It should be stressed again that this conclusion rests on the assumption of a sufficient value for a relatively uncertain quantity: a pervasive intergalactic ultraviolet flux. If current estimates of that quantity were to be found too high, column densities of HI in the outskirts of galaxies and in diffuse clouds outside of disks would have to be revised.

We address next the validity of the assumption of optical transparency. That assumption is invalid in a number of cases: dense regions of the interstellar medium, whence originate absorption lines, are opaque. The integrated line profile of a galaxy results from the collective emission - and absorption - by all its HI. In order to correctly convert the line integral into a total HI mass, we need to know the fraction of the HI gas in the disk which is found in optically thick regions. That fraction in turn depends on the intrinsic properties of the gas distribution in the galaxy and on the geometrical perspective with which it appears to us. The practical approach to this problem consists in computing column densities in the optically thin approximation and then applying a correction that accounts for self-absorption. The self-

absorption correction can be estimated (a) from statistical studies on large samples of galaxies, covering a broad range of disk inclinations and morphological and possibly luminosity class, (b) from HI absorption line studies in our Galaxy, or (c) by modeling the distribution of cold gas in the interstellar medium. A detailed description of these methods is given in Appendix B of Haynes and Giovanelli (1984). The results indicate that when a disk like that of our Galaxy is seen face-on, the assumption of optical transparency leads us to underestimate the column density by a small amount, probably less than five percent. When disks are seen close to edge-on, however, substantial corrections to the column densities and masses inferred using Equation (12.2) become necessary. The corrections appear to be larger for intermediate-type spirals. It is estimated that for the majority of galaxies, such column density corrections amount to factors less than 1.5.

If the distance is known, the total HI mass of a galaxy can be obtained by integrating Equation (12.2) over the effective disk area (i.e., the approximate ellipse obtained by the inclined view of the disk with respect to the line of sight), after correcting for self-absorption. In the case of single-dish observations where the galaxy is unresolved by the beam, Equation (12.2) yields simply

$$M_{\mathrm{H}} = 2.356 \times 10^5 d^2 \int S_c(v) dv M_{\odot} \qquad (12.3)$$

where d is the distance in Mpc and $\int S_c(v)\, dv$ is the integral, over the line, of the flux density corrected for self-absorption and other instrumental biases, with $S_c(v)$ expressed in Jy and v in km s^{-1} [see Roberts (1975) for details of the derivation of Equation (12.3)].

Standard radio spectroscopy techniques allow for spectral resolutions better than 0.1 km s^{-1} at 21 cm. Extragalactic observations are however preferentially done with broad bandwidths, covering typically 2000, 4000, or 8000 km s^{-1}; spectral resolutions are then more typically on the order of 5 to 20 km s^{-1}, although they can be much better than that when the signal strength so permits. The fine spectral resolution achievable in the HI line ordinarily allows very precise measurements of radial and rotational velocities of large samples of galaxies. In face-on systems, accurate measurements of the velocity dispersion of the interstellar gas perpendicular to the plane of the disk are possible. In inclined systems, the determination of the disk velocity field allows a detailed study of the large-scale galaxian dynamical characteristics. The maximum rotational velocity, as indicated, for example, by the half-width of a galaxy's integrated line profile, has been found to be a good luminosity indicator, thus providing a powerful method for the determination of extragalactic distances and hence the expansion rate of the universe.

The HI content of a galaxy has been shown to be vulnerable to environmentally driven gas removal mechanisms, and may thus be used to probe the effects of the latter on galaxy evolution. The fragile outer layers of the disk are easily disrupted by close encounters of galaxies, especially of those located in small groups, and HI observations have provided spectacular data on this sort of perturbation. As for the physics of disks, HI observations provide valuable insights on the dynamic and thermal equilibrium

of the interstellar medium.

In addition, the combination of large apertures and modern receivers has made the execution of large-scale redshift surveys in the 21-cm line a practical endeavor.

Spiral galaxies within 100 to 200 Mpc are easily detectable in the line with modest investments of telescope time, yielding recessional velocities with errors of only a few km s^{-1}. While optical redshift surveys preferentially favor objects of high central optical surface brightness, galaxies of low optical surface brightness tend to have abundant HI and, at equal apparent magnitude, are more easily detected by radio surveys. For example, while redshifts of galaxies in clusters - where lenticular and elliptical morphologies are most abundant - are usually obtained by optical means, the vast majority of redshifts available for galaxies in the low-density regions of superclusters have been obtained using radio methods.

12.1.3. Pictorial Presentation of HI Data

In the best cases, the body of HI data on a galaxy can be thought of as a three-dimensional array of intensities, expressed in terms of two angular coordinates in the plane of the sky and radial velocity, which may be referred to as a "data cube." The array values are set by the six-dimensional position-velocity distribution of the galaxian HI. In an idealized form, one can assume that the HI is confined to a thin disk and that axial symmetry holds for both its distribution and velocity field. In panels (a) and (c) of Figure 12.1, both the radial dependence of the HI surface density and the rotation curve are idealized averages of those observed in intermediate-type spirals. Integration of the data cube along the radial velocity axis will yield a map of the column density distribution in the sky; in panel (b) of Figure 12.1, the disk is simulated at a viewing inclination of 60°. The degree of shading represents the column density map. Each member of the superimposed family of lines identifies the locus of points characterized by a constant radial velocity. If instead of integrating over radial velocity, we slice the data cube at a constant value of one of the sky coordinates, for example, slightly off and parallel to the major axis of the tilted disk, we obtain a position-velocity map (d) which mimics the rotation curve (b), blurred by the limitations of spatial and spectral resolution. A slice of the cube at constant velocity will yield a "channel map," as in panel (e): the angular distribution of all galaxian HI whose velocity falls within a narrow velocity range, for example, the span of a single receiver channel, now mimicking one of the loci of panel (b). Finally, observation of the galaxy with a single dish that does not resolve the HI disk will yield an integrated profile of the type shown in panel (f). Of course, real data will be cursed (or blessed ...) with asymmetries, spiral features, small-scale irregularities, flared or disrupted disks, etc. Sub-arcminute-resolution HI maps are now available for several dozen galaxies, and single-dish profiles for approximately 6000. A catalog of extragalactic HI observations (Richter et al. 1983) is maintained, updated, and available to the astronomical community.

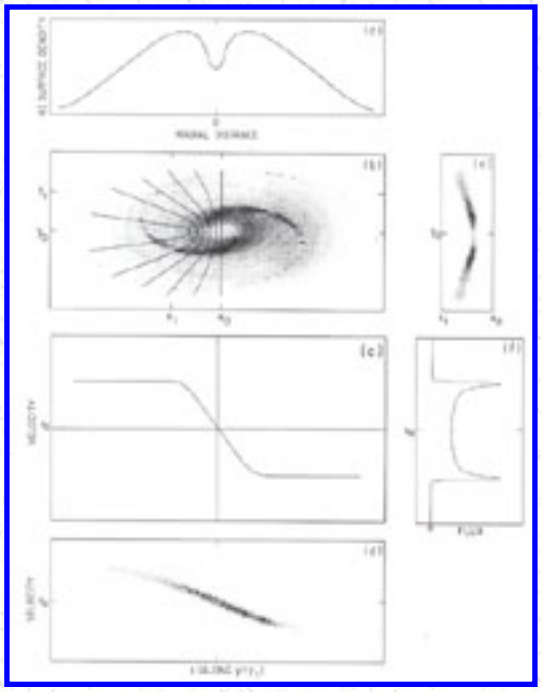

Figure 12.1. Pictorial representation of HI data. Panel (b) simulates the distribution of HI in a galaxian disk inclined 60° with respect to the plane normal to the line of sight; the shade intensity is visualized as being proportional to the HI column density across the disk. Superimposed on the left part of the image is a family of curves which identifies isovelocity contours. Because this is a symmetric idealized representation, isovelocity contours on the right part of the galaxies are mirror images of those on the left. Panel (a) illustrates the azimuthally averaged HI surface density, as a function of distance from the center of the galaxy. Panel (c) describes the rotational velocity of the galaxy, as measured along the major axis $y = y_0$; correction of this function by a factor 1 / sin i, where i is the inclination (60° here) of the disk, yields the galaxy's rotation curve. The systemic velocity of the galaxy is V_0; the straight, vertical isovelocity contour in panel (b) identifies the locus of points at $V = V_0$.

A slice of the galaxy along $y = y_1$ gives a position-velocity map as in panel (d), which in shape (but not in slope) mimics the curve in panel (c); again, intensity of shade is proportional to column density; the smoothing effects of a nonzero angular and spectral resolution have been introduced and are responsible for the breadth of the region with significant emission in panel (d). A "moment map" (or a "channel map"), i. e., the surface density distribution of HI within a narrow-velocity interval (e.g., a single spectral channel) is illustrated in panel (e); the chosen velocity interval in panel (e) corresponds roughly to that between the second and third isovelocity contours plotted in panel (b). Finally, panel (f) shows a spectrum of the whole galaxy, as seen by a single dish that cannot resolve its HI disk.

12.2. THE DISTRIBUTION OF HI IN GALAXIES

12.2.1. Morphology

As mentioned in Section 12.1, the optical morphology of a galaxy certainly bears some relevance to the HI content and distribution, but it is important to remember that the optical light and the HI emission do not necessarily arise from the same locations. Most of the detected HI in our own galaxy represents a galaxian population clearly associated with the disk but not coextensive with other conspicuous large-scale components of the interstellar medium, such as molecular clouds or HII regions. The neutral, atomic hydrogen is typically found farther out in the disk than any of its other directly measurable components.

The HI distribution in galaxies with a well-established disk in the stellar component is also disk-shaped. The outlines of spiral arms are often conspicuous in the HI gas, as beautifully illustrated by the two-armed spiral pattern of the map of M81 of Rots and Shane (1975). In nearby galaxies for which the linear resolution of observations is particularly high, details that bear on the structure and dynamics of the interstellar medium are discernible. For example, in the case of M31, bubblelike features are observed, with sizes ranging from the map resolution limit (80 pc) up to 1 kpc (Brinks and Bajaja 1986).

A notable aspect of galaxian HI disks is the occurrence of strong central surface density depressions.

Such depressions tend to appear more conspicuous in high-luminosity early-type spirals which possess large bulges. In lenticular galaxies the central depressions are frequently larger than the optical disks themselves, in which case the term "HI disk" tends to be modified to "HI ring." Although these outer HI rings are usually concentric with the optical disks, they can be strongly inclined to the latter. The azimuthal distribution of HI within the rings can be rather irregular, to the point that segments of the ring may not even be detected. In some S0's, diffuse polar rings are seen, orthogonal to the plane of the normal stellar disk, and are occasionally rich in HI. The trend of central depressions growing with earlier optical morphology is not entirely systematic, as summarized by van Woerden et al. (1983). The presence of the central depression in M31, an intermediate spiral, can be appreciated in Figure 12.2; notice how in M31 the region dominated by the stellar bulge is nearly devoid of HI. In our galaxy, the HI surface density starts to decrease at approximately the radius at which that of molecular hydrogen reaches a peak. In the case of early-type disks, not enough molecular gas is found to compensate for the locally anemic HI distributions. At the other extreme of the Hubble sequence, irregulars and gas-rich dwarfs exhibit an HI distribution similar in character to that of their light: clumpy and disorganized.

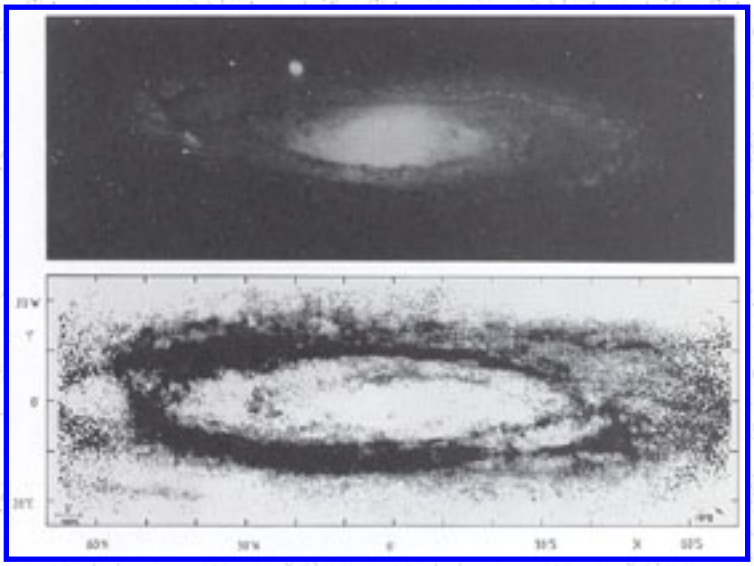

Figure 12.2. HI distribution in the disk of M31, obtained by Brinks and Bajaja (1986) with the Westerbork Synthesis Radio Telescope; the linear resolution on the plane of the sky is about 80 pc.

A frequently used azimuthally symmetric model for the HI surface density $\sigma_H(r)$ which gives a useful rough representation for most spirals is the sum of two Gaussians, the inner one with amplitude and width respectively -0.6 and 0.5 of the corresponding values for the outer one. This simplified model glosses over individual details and asymmetries and some large-scale features that may be common to most spiral disks. Sancisi (1983) has shown that a common feature seen in the outer regions of spirals is an HI "shoulder": a steep drop in $\sigma_H(r)$ occurs usually near the optical radius (normally the "Holmberg radius" at 26.5 mag arcsec^{-2}), followed by a gentle decrease at larger radii. Such shoulders are especially noticeable among galaxies that have very extended HI distributions. The onset of warps (see Section

12.2.3) tends to coincide with the "shoulder" radius. Gas in the shoulder may differ dynamically from the inner HI, being characterized by offset eccentric orbits instead of circular ones, and may form an envelope to the whole galaxy. Sancisi thinks that very large HI rings, as seen in lenticulars, may represent extreme examples of "shoulders." Interpretations of those features in evolutionary terms are not widely accepted. In special cases, episodes of accretion of gas-rich systems by a dominating galaxy are invoked, as in the case of polar rings. However, the relatively frequent occurrence of some features-such as the "shoulders" described by Sancisi, which have in several instances been observed to begin at a truncation edge of the stellar disk-suggests that internal causes should perhaps be sought within the framework of a slowly infalling disk model or of one where at some critical radius the onset of dynamical instabilities precipitates noncircular motions.

12.2.2. Sizes

The "size" of a galaxy as seen in HI is usually equated with the diameter of the furthest detectable HI isophote; this definition leads to a measurement which increases as observing hardware improves. Currently, routine observations of galaxies with synthesis instruments reach column densities of 1.0×10^{20} cm^{-2}. With large, single dishes (mainly the Arecibo 305 m), mapping of large-angular-diameter galaxies to column densities of 2.0×10^{18} cm^{-2} has been obtained, albeit with limited angular resolution and for relatively few objects. A limiting factor in high-sensitivity measurements with single dishes is the contamination by radiation collected by sidelobes of the antenna beam; while well understood, this contamination can be difficult to remove at very low HI surface density levels if bright HI emission is found just outside the field of interest. In the absence of such sources, however, measurements to 5.0×10^{17} cm^{-2} can be reliably conducted. Systematic analysis shows that the size of HI disks, like the integral HI content, is dependent not only on the internal characteristics of the galaxy, but also on its environment, as discussed in Section 12.6. The outer regions of a disk are very fragile and can be severely affected, thermally or dynamically, by a violent environment. When statistical properties of HI distributions are mentioned, it should be assumed that they refer to relatively unperturbed systems. In addition, it should be kept in mind that relatively low column densities of HI may become undetectable. To see that, note first that typically, for a given line width, the HI column density is proportional to the line brightness temperature. However, as seen in Section 12.1.2, if the opacity of the gas becomes very low, the fractional deviation of the spin temperature from the 2.7 K of the microwave background, $(T_S - 2.7) / T_S$, is depressed. For a given column density, then, the line brightness temperature diminishes in the same measure, as described by Equation (12.2) and discussed in more detail by Watson and Deguchi (1984).

More readily obtained estimates of the size of the HI distribution are those which express it as an isophotal or as an effective radius, the latter identifying the radius within which a fraction of the total HI mass is contained. When expressed in terms of the isophote at $N_H = 1.82 \times 10^{20}$ cm^{-2} the average ratio of the HI to the Holmberg radius is about 1.5; alternatively, 70% of the galaxy's HI mass is contained, on average; within 1.2 Holmberg radii. Dependences of HI radius on morphological type are very weak and difficult to discern; the distribution of sizes around the mean is strongly skewed, relative to the Gaussian. For reasons that are very poorly understand, some galaxies exhibit enormously extended HI

disks. Notable are the cases of Mk 348, illustrated in Figure 12.3, and of NGC 628, in which HI is detected out to several Holmberg radii. In the nearby system M33, HI is detected out to three Holmberg diameters. The exceptional HI objects are not systematically unusual in any other respect. Still, the incidence of very large HI disks has important implications. Dynamically, it allows inspection of the gravitational potential of a galaxy at very large distances from its center; from a cosmological viewpoint, the "intervening galaxy" explanation of high-redshift absorption lines seen along the line of sight to QSOs demands large cross sections of the intervening galaxian disks in order to account for the number of such lines observed (see Section 12.7.4). Huchtmeier et al. (1981) have noted that a significant fraction of irregular galaxies contain extended HI components not correlated with their optical size; the role of the extended gas component in the evolution of a galaxy is however still unclear.

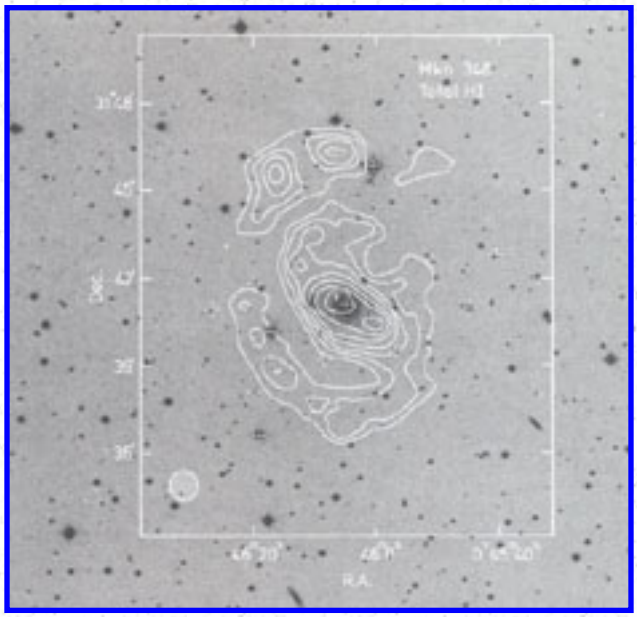

Figure 12.3. HI distribution in Mk 348, obtained by Heckman et al. (1982) with the Westerbork Synthesis Radio Telescope. Reprinted with permission from the Royal Astronomical Society.

12.2.3. Warps

The outer regions of the HI distribution of galaxies tend to exhibit strong departures from the regularity usually seen in the inner regions. It has been known for decades that the plane of the Milky Way displays an elegant hat-brim effect; the deviation of the centroid of the outer disk from the plane defined by the inner disk reaches 1.5 kpc at r = 18 kpc from the center. This effect was long attributed to a close tidal encounter with the Magellanic Clouds. However, perhaps the most spectacular example of a warp in another galaxy occurs in NGC 5907, displayed in Figure 12.4, which has no visible nearby neighbor that could serve as perturber. In addition, the galactocentric azimuth of the maximum height of the warp in our galaxy does not appear to depend on galactocentric distance, i.e., the warp does not precess under galactic rotation. This condition suggests the existence of self-maintaining mechanisms. A large fraction

of the edge-on galaxies mapped in HI show evidence of warps. The onset of a warp usually coincides roughly with the Holmberg radius of the disk; the optical light also often falls steeply past this point. The warp of NGC 5907 shows only in the HI disk; in the case of NGC 4565, however, a slight warp is also observed in the stellar disk. While warps are easy to detect in maps of the HI distribution in edge-on galaxies, they can also be inferred from the characteristics of the velocity field in more face-on disks. Deviations from circular rotation, associated with the gas in warps, produce characteristic signatures in isovelocity contour maps. Warps thus identified are referred to as "kinematic" warps. Examples of kinematic warps are illustrated in some of the panels in Figure 12.7 and discussed in Section 12.3.2. A review of the theoretical problems associated with the interpretation of warps is given by Toomre (1983).

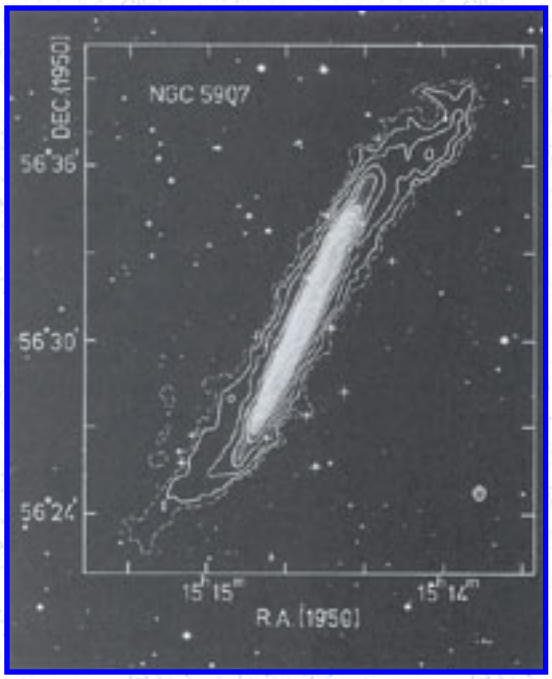

Figure 12.4. HI warp of NGC 5907, as observed by Sancisi (1976) with the Westerbork Synthesis Radio Telescope.

12.2.4. Appendages

In nearby loose groups of galaxies, HI appendages are often seen to extend outward from the disks of member galaxies: peninsular "plumes" and "tails," connecting "bridges" and other such features. A number (but not all) of these HI appendages have been explained in terms of tidal interactions among neighboring galaxies. In the Local Group, the linear feature known as the Magellanic Stream is probably the result of tidal forces in the Milky Way-LMC-SMC system. Examples of HI tidal streams which have been successfully modeled include those seen in the systems NGC 4631/56, NGC 4038/9, and M81/M82/NGC 3077. Figure 12.5 shows the HI distribution in the Leo triplet NGC 3623/7/8 obtained at Arecibo. In this example, the overall characteristics of the observed HI distribution can be well reproduced by the interaction caused by postulating a hyperbolic passage of NGC 3627 past its neighbor NGC 3628 with a perigalactic distance of about 20 kpc. The disruption caused to NGC 3627 is much reduced because the

sense of its orbital motion is opposite to that of its rotation; in NGC 3628, on the other hand, the two vectors are aligned and the damage is more severe, resulting in the conspicuous tail drawn mainly from the periphery of that galaxy. NGC 3623 has not recently had a close interaction with the other two.

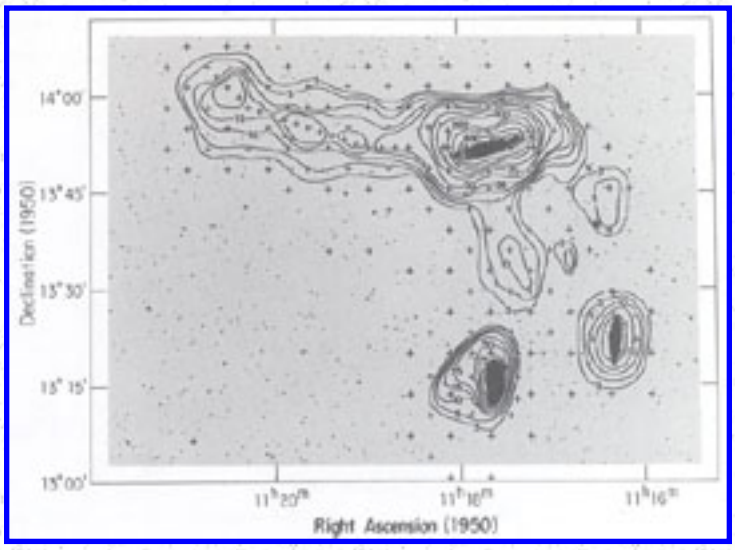

Figure 12.5. HI distribution in the Leo triplet of galaxies - NGC 3623, NGC 3627, and NGC 3628 - obtained with the Arecibo 305-m reflector by Haynes et al. (1979). Angular resolution of the map is 3.3'. The contours are of neutral hydrogen column density in units of 3.1×10^{18} cm^{-2}.

Several systems which contain substantial amounts of HI outside of galactic disks are less easily modeled as transient phenomena. Stefan's quintet (Shostak et al. 1984) is a group of five objects located close together on the sky. One of the galaxies is likely to be in the foreground; the other four lie at the same redshift and are morphologically peculiar. In fact, the HI at the velocity of the suspected foreground galaxy is regular while at least three distinct velocity systems are seen at the higher redshift. The bulk of the HI at the higher velocities lies outside the optical boundaries of any of the remaining quartet, and it appears that tidal and collisional stripping among those galaxies have succeeded in removing the majority of the disk gas from the participants. An even more perplexing case is found in the ring of HI found in the multiple group dominated by M96 and M105, also in Leo (Schneider et al. 1986).

12.3. VELOCITY FIELDS

12.3.1. Rotation Curves

The term "rotation curve," as applied to spiral galaxies, refers to that function $V(r)$ that describes the tangential velocity in the plane of the rotating disk, in terms of the distance r from. the galactic center. Most of the observational work on rotation curves of disk galaxies has focused on using the interstellar

gas as a tracer of the gravitational potential produced by the total content of the galaxy, i.e., stars, gas, dust, radiation and dark matter. Until about ten years ago, the bulk of the rotation curve data was derived from optical observations of the narrow lines emitted by HII regions; such lines are easily detected in star-forming regions of disks. Bright HII regions, however, while relatively conspicuous in the inner parts of disks, become rare in the outer regions. HI gas, on the other hand, typically extends with detectable column densities beyond the outer boundary of the HII region distribution, so that velocity measurements from HI maps provide the rotation curve and, by inference, the mass in the outer parts of spiral galaxies. Luminous galaxian material fades exponentially with radial distance, and until the early 1970s, it appeared reasonable to expect that the luminous matter was a good tracer of the total mass. Therefore, rotation velocities were expected to start falling in the periphery of luminous disks, as a result of the corresponding decline in mass density. If the mass of a galaxy were strongly concentrated, one would in fact expect the rotation curve to approach asymptotically a Keplerian $r^{-1/2}$ decrease. Seminal work on the stability of disks, which invoked the presence of massive, dark halos, and early single-dish 21-cm measurement of large nearby galaxies indicated the fallacy of such an expectation.

Many rotation curves have now been measured well outside the optical disk. Perhaps the most interesting characteristic of the HI rotation curves is that the rotational velocity does not fall even at large distances from the center, as can be appreciated in Figure 12.6, showing several examples obtained by aperture synthesis observations. In practice, both optical and HI line measures are used in studying rotation curves. Optical spectra outline the rotation in the bright inner disk while the velocity field in the outer portion is derived from 21-cm mapping.

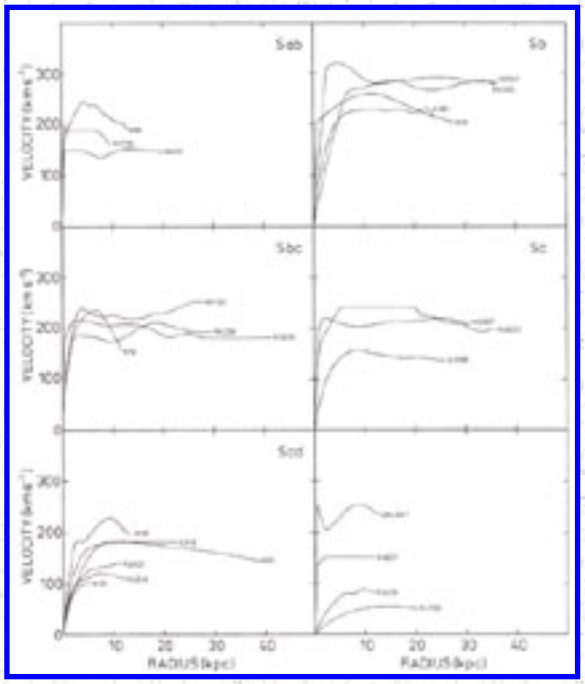

Figure 12.6. Selection of rotation curves of spiral galaxies, assembled by Bosma (1981). (Reprinted with permission from The Astronomical Journal).

Given the rotation curve $V(r)$, simple balance of gravitational and centrifugal force in spherical symmetry gives for the total mass $M_T(r)$ contained within r

$$M_T(r) = 2.33 \times 10^5 r V^2(r) M_\odot \qquad (12.4)$$

with $V(r)$ in km s^{-1} and r in kpc. [If the assumption of spherical symmetry for $M_T(r)$ is relaxed, the constant in Equation (12.4) diminishes slightly.] A rotation curve which becomes flat in the outer regions implies a linearly rising $M_T(r)$ and a mean density that decreases as r^{-2}; since the luminous matter decreases exponentially, the ratio of dynamical to luminous mass grows with r. In general, rotation curves of spiral disks remain flat, or perhaps rise very mildly as $r^{+0.1}$ at large radii. The maximum rotational velocity reached within a disk, V_{max}, is a function of both luminosity and morphological type. For a given type, higher peak rotation velocities - as derived from long-integration optical measurements - are attained by brighter systems. At a fixed luminosity, earlier spirals are faster rotators than late ones. (The largest rotational velocity observed thus far in a disk is about 500 km s^{-1} in the S0a galaxy UGC 12591.)

The correlation between luminosity and V_{max} is of the form

$$L \propto V_{\rm max}^n \qquad (12.5)$$

with n close to 4. In Section 12.4, we discuss the use of HI profile velocity widths in applying Equation (12.5) to estimate luminosities, and hence redshift-independent distances. Equation (12.5) can be derived from simple empirical and scaling relations, as shown by Aaronson et al. (1979). In addition, Faber (1982) finds that Equation (12.5) provides insight into a question of cosmological importance. Her reasoning is that as the rotational velocity at large radii is a dynamical manifestation of the total mass (which, to a large extent, is composed of spheroidally distributed, mostly nonluminous matter), it should be related to total mass in the form

$$M_T \propto (V_{\rm rot})^{12/(1-m)} \qquad (12.6)$$

where m is an integer whose value is determined by the exponent of the power law spectrum of primordial density perturbations. The relation in Equation (12.6) applies to hierarchically clustered, dissipationless structures, such as any spheroidal mass distribution. Assuming that a constant mass-to-luminosity ratio holds, at least for galaxies of a given morphological type, the empirical relation in Equation (12.1) with $n = 4$ determines the exponent of the power spectrum in Equation (12.6). One obtains a value for m of -2, which agrees with other independent estimates of m that set $m = -1$ as an upper limit. This result implies that the power spectrum of primordial density fluctuations is highly skewed towards large fluctuations relative to what one would expect for uncorrelated perturbations ("white noise"). Note that if m were independently well known, Equation (12.5) could be inferred from

Equation (12.6).

In the inner regions, rotation curves rise steeply; the scale length of that rise is inversely correlated with V_{max}, and consequently with the luminosity of the galaxy. The rise appears nearly linear, which is consistent with what one would expect, for example, for a rotating rigid body or homogeneous spheroid. In order to obtain detailed descriptions of $V(r)$, clearly both high spectral and angular resolution are necessary, especially in the inner regions, where $V(r)$ may have steep gradients. Often, however, there is little or no detectable HI in the inner regions-especially in early-type disks - which makes the measurement of $V(r)$ arduous. The combination of optical and radio techniques provides, in the majority of cases, the best means of carefully determining $V(r)$ throughout the disk. Good quality rotation curves are known for several dozen systems. Single-dish profiles of the type shown in Figure 12.1(f) are much easier to obtain and thus more common; from them it is possible to extract a value of V_{max}, which can then provide an indication of the total mass contained within the region observed in the HI line. Unless the galaxy is mapped, the exact extent of this region is unknown and the estimate relies on statistical considerations.

12.3.2. Distortions in the Velocity Field

In many galaxies the velocity field, as described in Figure 12.1(b), is observed to deviate from axial symmetry in such a way that the HI cannot be rotating in circular, coplanar orbits. Figure 12.7 illustrates the variety of observed velocity fields. M83 and NGC 5383 illustrate two kinds of deviation that maintain a sort of twofold symmetry in the velocity field. One of them, the kinematic warp, was briefly discussed in Section 12.2.3 and is exemplified by M83: a change in the position angle and inclination of the warp produces a characteristic S-shaped distortion. The same effect can also be discerned, although less dramatically, in NGC 5055 (see Figure 12.7). M31 is perhaps the system where the most detailed rendition of a warped disk is kinematically observable but it is by no means typical. As the inclination of the disk is high (about 77°), the line of sight can cross the disk in three different locations, including two in the upward and downward brim of the warp, yielding triple-peaked velocity profiles. A warp is a perturbation that involves the outer parts of the disk; the second kind of distortion, an "oval distortion," arises in the inner parts and results from structures that depart from the symmetry of the optical image of the outer regions of the disk, such as bars or ovals (i.e., "fat" bars). The resulting perturbation in the velocity field causes the major and minor symmetry axes in the inner parts of the galaxy not to be perpendicular, as can be seen in NGC 5383 in Figure 12.7.

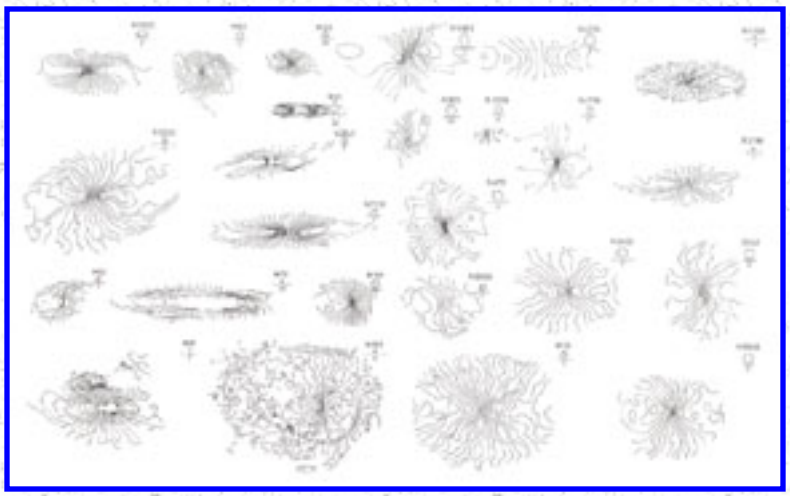

Figure 12.7. Selection of velocity fields of spiral galaxies, assembled by Bosma (1981). (Reprinted with permission from The Astronomical Journal).

12.3.3. The Mass Distribution in Spiral Galaxies

By combining optical photometry data with the mass derived from 21-cm observations via Equation (12.4), we can determine total mass-to-luminosity ratios - although one should note that values thus obtained depend inversely on the assumed distance scale. Arbitrarily choosing some limiting radius, e.g., r_{25}, measured at the blue isophote of 25.0 mag arcsec^{-2}, the integral of Equation (12.4) and the blue luminosity within r_{25} yield a measure of the global mass-to-light ratio. Using this system, Rubin et al. (1985) find that ratio to be *6.2, 4.5, and 2.6 for Sa, Sb, and Sc galaxies*, respectively, with an error on those mean values of about 10%. Since the mass is proportional to $r_{25}\ V_{max}^2$, and since it is found that, in the blue, the relationship between luminosity and radius is independent of morphological type, the variation in (M_T / L_B) with type is essentially one of V_{max} with type. The mean values of V_{max} as a function of type bear out that conclusion. The values of (M_T / L_B) are virtually constant within a given Hubble type, over a range of several magnitudes. Now, what fraction of the total dynamical mass does the luminous mass constitute? To answer that question, we must first obtain an estimate of the fraction of the total luminous mass represented by L_B. Work based on model stellar populations indicates that reasonable values for the ratio between the total mass in all stars and LB are 3.1, 2.0, and 1.0 for Sa, Sb, and Sc types, respectively. Although these numbers are relatively uncertain, they indicate that the ratio of total to luminous mass within the 25-mag arcsec^{-2}, isophote is likely to be on the order of 2 for spirals of all types. As the mass grows more or less linearly and the light fades exponentially, the mass-to-light ratio grows rapidly outwards from r_{25}.

The analysis of rotation curves yields information on the mass distribution as a function of distance from the galactic center, but none whatsoever on the distribution as a function of distance from the plane of the disk. One would like to know which fraction of the total mass resides in the disk and which in the halo, and also how the total mass-to-light ratio of the disk alone varies with radius. In order to answer these questions, it is necessary to measure the characteristics of some tracer of the gravitational potential

in the *z*-direction (i.e., perpendicular to the disk); handily, such is the HI. It is possible to obtain the distribution and the velocity dispersion, in the *z*-direction, of the galaxian HI. The former can be measured from high-resolution maps of edge-on galaxies, the latter from spectral profiles of isolated regions in face-on disks.

Following van der Kruit and Shostak (1983) and references therein, let us assume that a spiral disk can be approximated by a self-gravitating sheet which is locally isothermal (i.e., the velocity dispersion of any of its components is independent of *z*). Then the total mass density can be expressed as

$$\rho(r,z) = \rho(r,0)\,\mathrm{sech}^2\left(\frac{z}{z_0}\right) \tag{12.7}$$

where z_0 may be a function of the distance from the center (in the plane), *r*. The HI disk can be assumed to be effectively massless, in comparison with other dynamically important components; it can then be shown that the HI density decreases to half of its midplane value at a height z_H,

$$z_H = 0.85\langle v_z^2\rangle_H^{1/2}[2\pi G\rho(r,0)]^{-1/2} \tag{12.8}$$

where $<v_z^2>_H^{1/2}$ is the *z*-velocity dispersion of the gas and *G* is the gravitational constant. We can rewrite Equation (12.8) as

$$z_H(r) \propto [\langle v_z^2\rangle_H(r)]^{1/2}\left[\frac{M_d(r)}{L(r)}\right]^{-1/2}[L(r)]^{-1/2} \tag{12.9}$$

where $M_d(r)$ is the disk mass within radius *r* and the luminosity profile $L(r)$ is obtained from major-axis photometry. Measurements of $<v_H^2>_H^{1/2}$ have been made directly in a few face-on galaxies; all yield values in the range of 7 to 10 km s^{-1} and appear to vary relatively little with *r*. One can thus apply Equation (12.9) to a well-mapped edge-on object, such as NGC 891 or NGC 7814, for which $z_H(r)$ is then known. By assuming a value of $<v_z^2>_H^{1/2}$ as measured in face-on spirals, and by photometrically determining $L(r)$, we can obtain the details of the (M_d / L) ratio within the disk. Such an operation yields the following results:

- The mass-to-luminosity ratio of the disk is independent of *r*, and hence the luminosity profile of the spiral disk is also a profile of the disk's mass.
- Only one-third of the total mass of NGC 891 within the distance to the edge of the optical disk actually resides in the disk itself, the rest being distributed in a much thicker component, the halo.

- At r = 10 kpc, the mass density of the disk at z = 0 exceeds that of the halo (assumed spherical) by a factor of 4; at r = 21 kpc, that ratio decreases to 2.

- In the edge-on Sab galaxy NGC 7814, only a small fraction of the total mass, interior to the optical radius of 22 kpc, is in the disk; its light distribution, furthermore, is dominated by the spheroidal bulge. The rotation curve then can be used to sample the bulge's mass-to-light ratio; it is found to increase by a factor of 10 between the inner regions (r < 10) and 22 kpc.

In conclusion, the dynamical masses of spiral galaxies are found to be still growing linearly beyond the edges of their optical disks, at least out to the greatest radii at which gravitational potential tracers like HI are detectable. Within the optical radius, no more than one-third to one-half of the mass resides in the disk. The ratio between luminous and dynamical mass within the disk is about constant with radius and independent of morphological type, while that of the spheroidal component grows rapidly with distance from the galactic center.

12.3.4. Dark Matter in Dwarf Galaxies

Although most of the galaxies that we see are of relatively high luminosity, it is not yet clear that they are in fact good tracers of the mass distribution. It is already known that low-luminosity galaxies are found to cluster less strongly than higher-luminosity ones (see Section 12.7.2). Since the number density of galaxies still rises at low luminosities, it is critical to understand whether the presence of dark matter - the so-called "missing mass" - is required to the same extent in the low-luminosity but numerous dwarf galaxies. In particular, we need to have some idea of whether these objects contribute more, less, or the same amount to the matter distribution as do galaxies of higher luminosity.

Dwarf counterparts of elliptical, lenticular, and irregular galaxies exist and are in fact the dominant population, by number, of the Virgo cluster. The presence of dwarf spiral galaxies is controversial, and an absence of low-mass spirals is predicted by some theories of the origin of spiral structure. While the dE's may be the most common galaxy in Virgo, dI's may represent the most widely distributed objects in the universe (see Section 12.7.2). Although dI's are typically of low optical luminosity and surface brightness, they also contain significant fractions of their total mass in the form of HI (Fisher and Tully 1975). Their global 21-cm profiles are often Gaussian rather than two-horned, indicating that random motions are significant and possibly dominant.

Recent synthesis observations have been made to investigate the HI distribution and velocity field of a number of very-low-luminosity dI's (Sargent and Lo 1986). The HI distributions vary from annular to totally without organized structure, but are generally larger than the stellar distributions. In all of the mapped dI's, the amplitude of the rotation curve is comparable to or smaller than the random velocity dispersion, and several of the objects show no sign of systematic velocity fields. While the kinematics of the brighter dI's (M_{pg} < - 14) tends to be dominated by rotation, the chaotic motions are more important at lower luminosities. While there is a trend that the HI fraction of the mass of the dI's rises with decreasing optical luminosity, the gas only rarely dominates the total mass. Still, in no case is the

rotation curve observed to turn over at large r; in most cases, the rotation curve is linear and still rising (solid-body rotation) even outside the optical image. It is difficult, if not impossible, to estimate the inclination of a dI, unless its velocity field is regular enough that the inclination can be derived from the best-fit kinematic model. Despite the resulting uncertainties in mass estimates, it is clear that in all cases, the total mass-to-light ratio M_T / L is high, in the range of 10 to 30: dI's have dark halos also.

Although true dwarf spirals do indeed seem rare, at least one low-luminosity Scd galaxy, UGC 2259, shows a symmetrical HI distribution and a regular velocity field indicating a flat rotation curve similar to that seen in more luminous spirals (Carignan et al. 1987). The interpretation of the mass distribution for this galaxy is model dependent, but even the assumption of a minimum-mass dark halo implies that at the optical (Holmberg) radius, the luminous disk and the dark halo contribute equal amounts of mass. Thus it appears that the ratio of nonluminous to luminous matter is independent of the Hubble type.

12.4. THE VELOCITY WIDTH AS A DISTANCE INDICATOR

It is well know that there is a tight correlation between galaxy morphology and angular momentum, dominated in spirals by rotation. As a distance-independent quantity, the velocity width can be used in conjunction with some other observable to estimate the distance to a galaxy via a method that does not involve the redshift. Comparison of this "luminosity distance" with that predicted from the redshift serves as a means of deriving the Hubble constant and in identifying deviations from a smooth Hubble expansion. Calibration of the method relies on the assumption of known distances to a few nearby galaxies, obtained via primary indicators such as variable stars.

12.4.1. The Velocity Width-Magnitude Relation

As discussed in Section 12.3.1, the maximum rotational velocity reached within a galaxian disk depends on the luminosity of the galaxy, as described by Equation (12.5). In 1977, B. Tully and R. Fisher were the first to realize that such a circumstance lent itself to the measurement of distance moduli. They expressed the relationship in the form

$$M_{pg} = -a \log W_c - b \qquad (12.10)$$

where M_{pg} is the absolute photographic magnitude, corrected for both the extinction by dust in our galaxy and by dust in the target galaxy itself. The latter is generally parameterized by an inclination and a morphological-type dependence. W is the velocity width of the 21-cm line profile, integrated over the whole solid angle subtended by the HI in the galaxy after correction by a factor (csc *i*), where *i* is the inclination of the galaxian disk to the line of sight. The coefficients *a* and *b* were initially found to be about 6.25 and 3.5, respectively. Numerous authors successively applied the method, but doubts were cast on the legitimacy of the application of Equation (12.10). Brosche (1971) noted that the maximum velocity width observed is different for galaxies of different morphological type; later, Roberts (1978) pointed out that the velocity width-magnitude relation depends strongly on the morphological type, a

result later confirmed by the detailed studies of systematic properties of rotation curves by Rubin and coworkers (1985). The slope of the relation, in fact, when considered for individual morphological types, is closer to 10; it was the combination of galaxies of several morphologies, each with a different offset *b*, which initially yielded a flatter relation. The offset between Sa's and Sc's is, according to Rubin et al., about 2 magnitudes, in the blue. Important contributions towards understanding the biases in the use of the velocity width-magnitude relation have been made by Bottinelli et al. (1986 and references therein), particularly in connection with the determination of the Hubble constant.

The sources of uncertainty in establishing values of *a* and *b* can be serious. The circumstance that optimizes the determination of W_c, i.e., high inclination, conspires to render more uncertain both the correction for internal extinction to M_{pg} and the determination of the morphological type, necessary to decide which values of *a* and *b* in Equation (12.10) should apply. Aaronson and coworkers first proposed in 1979 that most of the uncertainties associated with the inclination corrections are minimized if infrared rather than blue or photographic magnitudes are used. The interstellar extinction at 1.6 μm is practically negligible, and hence the uncertainty in the magnitude correction is practically eliminated. In addition, Aaronson and coworkers found no dependence in the coefficients of Equation (12.10) with morphological type, when the absolute magnitudes at 1.6 μm replace the photographic ones, and a reduced scatter about the best fit to the data. The quality of this correlation is illustrated in Figure 12.8, an infrared magnitude-velocity width plot for 306 nearby galaxies. Aaronson and coworkers have interpreted this apparently fortuitous and most convenient of circumstances as a natural consequence of using infrared magnitudes, given the properties of the stellar population they trace, but their interpretation has been disputed by Burstein (1982). Rubin et al. (1985) find that Equation (12.10) is not independent of morphological type even at infrared wavelengths. As with blue magnitudes, the slope of about $a = 10$ is virtually independent of type, but an offset of about 1.3 magnitudes separates Sa's from Sc's. They also find that the scatter in the relation is not significantly reduced (rms of 0.68 with blue magnitudes, 0.67 with infrared magnitudes) by adopting 1.6 - μ magnitudes. The differences between the results of Rubin et al. and those of Aaronson et al. probably reside in different biases inherent in the choice of samples.

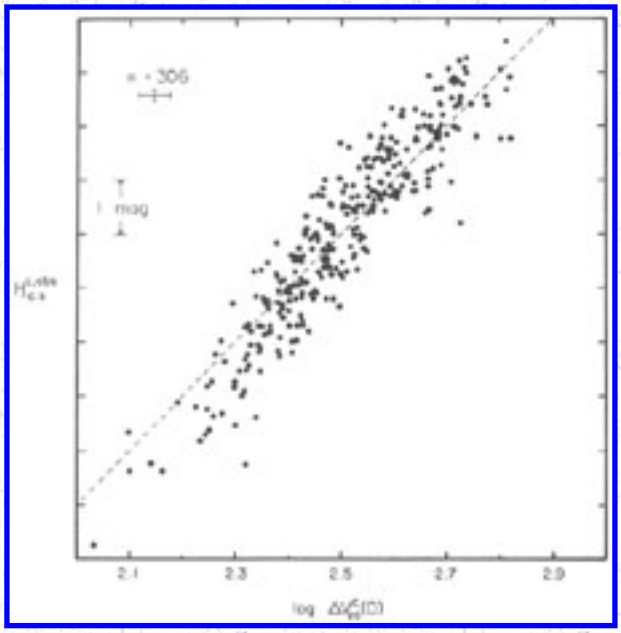

Figure 12.8. Infrared magnitude-velocity width relation for 306 nearby galaxies, after Aaronson et al. (1982). Absolute magnitudes were calculated assuming a uniform Hubble flow. Dashed line has a slope of 10. Error bar represents the typical uncertainty for a single point, as estimated by the authors.

The question of whether the infrared version of Equation (12.10) is truly a single relation, valid for all spirals, remains open; the possibility that a second parameter, in addition to W_c (e.g., type), may be necessary to infer luminosities appears likely. There is general consensus that the slope of the relation is close to 10, both in the blue and in the infrared, when samples of a given type are chosen. The velocity width is also seen to correlate well with optical size and with the HI mass. Large samples of good-quality HI profiles are becoming available to distances in excess of 200 Mpc. The method relies on the absolute determination of distance for a small number of local calibrators, obtained with traditional means. The quality and number of these calibrators should dramatically improve after launch of the Hubble Space Telescope. As the wrinkles of the method are slowly smoothed away, the velocity width-luminosity relation may provide one of the best tools with which to measure the distance scale of the universe.

The physical basis for the velocity width-magnitude relation is poorly understood. (A possible interpretation was given in Section 12.3.1.) A similar relationship between the luminosity and velocity dispersion is seen among ellipticals, $L \propto \sigma^4$, with a third parameter, the integrated surface brightness, providing the needed scale length to minimize the scatter. Indeed, equilibrium disk models with constant surface brightness and constant mass-to-light ratio predict $L \propto V^4$, but the application to all real galaxies is not clear.

12.4.2. Deviations from Hubble Flow

Despite the current uncertainties in its application, the velocity width-magnitude relation has been shown to be a promising tool in the study of deviations from the smooth Hubble expansion. Once the relation is established for a certain sample of galaxies, a predicted redshift, V_p, can be estimated for each galaxy. V_p can then be compared with the observed redshift, V_0. Systematic variations over the celestial sphere of the residuals $V_0 - V_p$ imply a large-scale bulk flow. Hart and Davies (1982) have used HI observations of nearby Sbc galaxies to determine the motion of the Sun and the Local Group relative to the more distant galaxies. Their method uses the HI mass as the standard candle for galaxies in this single Hubble type. Further extension of this technique to larger distances will investigate the scale over which peculiar motions can be measured beyond the boundaries of the Local Supercluster.

The velocity width-infrared magnitude method has also been used to derive relative distances to nearby clusters of galaxies. Since the galaxies in an individual cluster can be assumed to be at the same distance, a determination of the relation for galaxies in separate clusters yields a measure of the Hubble ratio (velocity/distance) for each cluster. Aaronson et al. (1986) have derived Hubble ratios for ten nearby clusters; the scatter in their results again implies significant deviation of the Local Group motion from what would be expected if the local Hubble flow were simply a smooth expansion.

It is clear that future refinement of this technique will provide a critical link in our understanding of the magnitude and direction of the peculiar motion and the scale size of inhomogeneity in the local universe.

12.5. HI CONTENT AND OTHER GLOBAL PROPERTIES

The term "HI content" of a galaxy has often lent itself to some confusion. The simplest and most obvious meaning is the mass of HI within the entire galaxy. As with absolute magnitude, however, this quantity is usually uncertain by a factor that goes with the square of the assumed distance scale. The ratio of the hydrogen mass to optical luminosity, M_H / L, being equal to the ratio of the related fluxes, is conveniently distance independent, and the label "HI content" has frequently been applied also to this quantity, contributing a measure of ambiguity. Here we shall maintain the term for the total HI mass, M_H, or, more properly, for the scaled quantity $h^2 M_H$, where h is related to the distance scale parameter in the form $H_0 = 100\ h$ km s^{-1} Mpc^{-1}. Remember that the total mass, derived from the maximum rotational velocity and a disk radius, scales linearly with h, and hence we will utilize the quantity $h M_T$. In this section, we will address the following question: how do global properties of a galaxy which are inferred from 21-cm observations, i.e., $h^2 M_H$, hM_T, and the scale length of the HI distribution, correlate with global properties, such as luminosity, linear size, and morphological type, which are measured at other wavelengths? A caveat is necessary at this stage: it has been found that the relationships between those parameters which are intrinsic to a galaxy's structure are not unambiguously defined, unless account is taken of the peculiarities of the environment surrounding that galaxy. Galaxies that live in high-population-density regions exhibit notable deviations in their behavior and possibly in their evolution. In Section 12.6, we discuss the evidence that such perturbations occur. Here we will discuss

the properties of unperturbed galaxies - those that have most likely spent their entire existence in relative isolation - and will assume, somewhat arbitrarily, that they define the standards of normalcy.

12.5.1. Relations Between Global Properties for Spirals (Sa and Later)

Derived from the sample of isolated galaxies of Haynes and Giovanelli (1984), Table 12.1 lists the average values of $\log(h^2 M_H)$ separately for various morphological-type groupings. The units of mass and luminosity are solar; the units of diameter are kpc and the errors are the standard deviations appropriate for individual objects in each sample (not for the mean). The number of objects used in each determination is also given. The HI mass, like other global properties of galaxies within a morphological-type group, exhibits wide variations that correlate reasonably well with blue luminosity, and less so with near-infrared ones. The scatter about the mean values of the ratio between HI mass and blue luminosity is reduced, with respect to that about HI mass means alone. As shown in Table 12.1, these two parameters exhibit variation not only within a single morphological class but also between different classes. For example, the M_H / L_B, ratio is about twice as large for Sc's as for Sa's. However, the difference between these mean values for even the two extremes of spiral morphology (Sa, later than Sc) is only of the same order as the rms scatter within the various type groups. This large scatter is intrinsic to each statistical grouping, not the result of measurement errors. It arises in part because integrated luminosities contain the contributions of both a disk stellar component and a bulge, which are quite different from both a dynamical and an evolutionary, viewpoint; the HI mass, on the other hand, is strictly a disk, extreme Population I component. Galaxies with widely different disk-to-bulge luminosity ratios coexist even within groups of objects sharing the same morphological label. The size of the major axis of the optical image of a galaxy, on the other hand, most likely represents a disk property, and one may expect a tight correlation with the HI mass. The logarithm of the ratio of the HI mass to the square of the linear blue major diameter, also a distance-independent ratio, exhibits a much reduced scatter about the mean for each type grouping, as listed in Table 12.1. In addition, the strong morphological-type dependence seen in M_H / L_B averages is greatly reduced. Involving as it does an HI mass and an optically defined surface area, the MID' ratio is a hybrid form of mean HI surface density. As discussed in Section 12.1, there is little evidence for a morphological-type dependence of the ratio between HI and blue radius; thus; the relative type independence of M_H / D^2 suggests that the mean surface density of HI is nearly invariant (within a factor of 2) among spiral galaxies.

Table 12.1. Average global properties.

Type(s)	N	$\log(h^2 M_H)$	$\log(M_H / L_B)$	$\log(M_H / D^2)$
Sa, Sab	38	9.37 + 0.47	-0.55 ± 0.41	6.69 + 0.32
Sb	74	9.67 + 0.42	-0.44 + 0.37	6.83 + 0.26
Sbc	38	9.54 + 0.43	-0.32 + 0.32	6.85 + 0.19

Sc	72	9.40 + 0.40	-0.28 ± 0.31	6.79 ± 0.19
> Sc	40	8.93 + 0.73	-0.04 + 0.33	6.87 + 0.17

HI content can also be measured as a fraction of the total dynamical mass, the latter as obtained from the inclination-corrected HI velocity width and an assumed width-mass relation (the rotation curve). The mean values of this ratio for the various morphological classes are not well determined. Inclinations are sometimes difficult to estimate, samples are reduced by the exclusion of nearly face-on galaxies, and the adoption of standard rotation curves to estimate total masses may be inappropriate for very late galaxies (such as dwarfs and irregulars), the gravity of which may be balanced by disordered, random motions rather than by rotation. Despite these caveats, the HI-to-total mass ratio varies between about 1.3% for Sa galaxies and 2.2% for Sc's, more or less monotonically through the Hubble sequence. The dispersions around these mean values are rather large, on the order of a factor of 2, comparable with the difference between mean values at the extremes of the spiral sequence. Because the current data do not conclusively indicate that the HI-to-total mass ratio is either type invariant or a good discriminator among the spiral classes, this ratio is not presently as useful an observational parameter reflecting HI content as M_H / D^2.

12.5.2. Content of Early-Type Galaxies

Elliptical galaxies are usually not detected in the HI line, even at sensitivity levels of a few mJy. While this may not be totally unexpected, as their stellar content is old and their angular momentum low, some gas should be present as a result of mass loss from aging stars and perhaps even more so in the fraction of ellipticals that appear to have dust lanes, central HII regions, or active nuclear sources that might result from gas inflow. In fact, some detections of HI in ellipticals have been obtained. Figure 12.11 illustrates one such detection, that of NGC 1052. Sanders (1980) proposed that the HI content of E's is bimodally distributed: most E's contain little or no gas, while a few are gas rich. Weighing carefully the information content even of non-detections, Knapp et al. (1985a) have analyzed a much larger sample - approximately 150 objects, of which 23 were detected - and have concluded that the ratio $k = (M_H / L_B)$ is distributed for ellipticals roughly as

$$\log[N(k)] = -1.9(\pm 0.2) - 1.48(\pm 0.13) \log k \qquad (12.11)$$

where $N(k)\, dk$ is the number of objects with (M_H / L_B) between k and $k + dk$. Note this distribution is *not* bimodal. This behavior is very different from that of spirals, which are generally distributed rather in Gaussian fashion than according to a power law. The concept of a "typical" value of M_H / L_B for ellipticals may thus be meaningless. The distribution of HI content for spirals and its correlation with disk properties indicates a tight relationship between the gas and the stellar population; on the other hand, the light of the elliptical bulges and the HI content of E's have little regard for each other. Knapp and coworkers suggest that the HI in E's has an external origin, obtained by accretion of a surrounding

envelope or of a gas-rich companion. This proposal is also supported by the tendency for the HI, when found, to be located well outside the optical image of the galaxy and to be characterized by peculiar kinematics.

While it is generally accepted that in the more luminous ellipticals, the HI gas has an external origin and is not produced by evolutionary stellar mass loss, the origin of HI disks in low-luminosity galaxies has been more controversial. Further evidence that the cool gas seen in all ellipticals comes from a source other than mass loss from the stars seen in the optical image is offered by VLA observations of the HI distribution and kinematics in four low-luminosity ellipticals (Lake et al. 1987). The velocity field of these galaxies is roughly regular, implying the presence of a rotating disk. In the brighter two galaxies, the HI distribution is annular; in the fainter two, it is centrally concentrated. In all four cases, however, the HI emission extends to twice the optical (Holmberg) radius. It is hard to see how such large HI disks could accumulate from stellar mass loss over a volume much large than the stellar component.

In the very nearby galaxies, even small amounts of atomic gas can be detected. VLA observations of the HI in the dwarf elliptical companions to M31, NGC 185 and NGC 205, show the presence of a few times 10^5 solar masses of atomic gas in contrasting configurations (Johnson and Gottesman 1983). Both galaxies show evidence of dust patches near their nuclei and small populations of blue, presumably young stars. In NGC 185, the centroid of the HI distribution is not coincident with either the nucleus or the dust clouds. On the other hand, the HI distribution in NGC 205, while elongated, reveals a rotating disk roughly coincident with the dust and blue star distribution. It seems that ellipticals in fact do contain small but measurable quantities of not only the atomic gas but also the expected associated quantities of dust derived from far-infrared observations (Jura et al. 1987).

The HI distribution in lenticular (S0) galaxies, recently reviewed by Wardle and Knapp (1985), appears to be intermediate between the cases of ellipticals and spirals. While S0a's appear to resemble spirals, in the sense that some properties of the stellar population are correlated with the gas content and that it appears sensible to estimate mean values of M_H / L_B and M_H / D^2, S0's are more like ellipticals. As for ellipticals, the values of k for S0's cover a very wide range and appear to be unrelated to the stellar population.

Knapp and Wardle propose that the HI in S0's may also have an external origin. Perhaps the strongest arguments in favor of such a hypothesis come from the special examples of the polar ring galaxies. These objects are otherwise-normal S0's, viewed edge-on and surrounded by tilted rings of luminous material. The current coexistence of two nearly orthogonal orbital planes suggests the formation of the ring by an unusual event, probably the capture of a gas-rich companion. Observations of the rotation curves of the ring material allow one to probe the *shape* of the dark halo surrounding these S0 galaxies (Schweizer et al. 1983). In combination with clues derived from optical spectroscopy and photometry, the derivation of the HI distribution and velocity field from synthesis maps determines an estimate of relatively young ages, about 1×10^9 to 3×10^9 years, for the observed polar rings. VLA maps are now available for several polar ring systems (van Gorkom et al. 1987). These objects appear to be relatively rich in HI, which is generally aligned with the ring rather than the S0 disk. Furthermore, the HI

distribution is sometimes asymmetric and extends well beyond the optical image, suggesting that there has not been enough time for the gas to settle into the ring or for the induced star formation to be completed. The S0's with neutral hydrogen rings but no optical counterpart may be more extreme examples of the same phenomenon (Knapp et al. 1985b). Although ellipticals and S0's are indeed found typically in regions of higher galaxy density than spirals, where the accretion or merger rate is expected to be similarly elevated, it is not yet clear that accretion of gas-rich companions can explain all seemingly anomalous cases of HI in early-type systems.

12.6. ENVIRONMENTAL EFFECTS

While some of the differences in the HI content and distribution observed in galaxies of separate morphological classes undoubtedly result from the circumstances of the era of galaxy formation, the present capacity of a galaxy for star formation may be influenced to some extent by its current environment. The content and distribution of the neutral component of a galaxy's interstellar gas serves then as a useful probe of possible external influences on galaxy evolution, as the neutral gas represents a long-lived but vital component for star formation. A recent review of this subject is given by Haynes et al. (1984).

12.6.1. Tidal Interactions

As illustrated in the tidal disruption model of the Leo triplet presented in Figure 12.5, close encounters between neighboring galaxies in loose groups can result in the removal of a significant portion-observed to be as high as 50% - of a galaxy's initial HI mass. Tidal models such as those presented by Toomre and Toomre (1972) illustrate two significant consequences of tidal encounters, consequences that may dramatically alter galaxy evolution. First, if the relative orbital angular momentum vector is at least roughly aligned with the rotational angular momentum of the target disk, then particle capture is enhanced by the prolonged tidal acceleration so that mass transfer from one galaxy to another occurs. Additionally, after the collision, gas either captured from the companion or raised to large *z*-heights above the plane may be gravitationally pulled back toward the bottom of the target's potential well. The removal of angular momentum from the gaseous component may even cause such gas to fall into the center of the galaxy. This gas influx may fuel nuclear activity; it is well known that many (although by no means all) active galaxies have close companions. Excess infrared and radio emission, indicative of a recent burst of star formation, is observed in obviously interacting galaxies. Such activity may be relatively short-lived. HI observations of active galaxies are discussed in Section 12.7.3.

Because the outer portions of a galaxy are those most likely to be disrupted in an encounter, HI makes an excellent tracer of tidal events. While ongoing tidal interaction can be inferred from observations of disturbed optical morphology, strong optical emission lines, and large infrared, radio, or X-ray flux, the details of an encounter can be more readily deduced from the HI spatial distribution and its velocity field. Cottrell (1978) has claimed that the coexistence of early-type stellar spectra implying recent star formation with colors characteristic of an underlying older population in Irr II galaxies is likely produced by binary collisions in which mass transfer occurs if at least one of the progenitor galaxies

contains a significant amount of interstellar gas. A number of nearby Irr II systems such as NGC 3077 and NGC 4747 show HI tidal tails. As mentioned in Section 12.5.2, mass transfer may play an important role in providing the HI presently seen in some elliptical and lenticular galaxies.

Although the density of galaxies is much higher in a rich cluster, the potential for dramatic tidal effects may be greater in loose groups. Since the tidal force varies as $1 / r_p^3$ and the effective duration of the encounter roughly as r_p / v_r, the "disruption damage" is just $1 / r_p^2 v_r$, yr in the impulse approximation, where r_p is the perigalactic distance and v_p is the relative velocity of the two galaxies. Because the typical velocity dispersion in a small group is much lower than that found in a rich cluster, a collision in a dense cluster will produce only about one-tenth the damage done by one with the same impact parameter and mass ratio in a small group.

12.6.2. Gas Deficiency in Cluster Spirals

Although tidal encounters may not appear as dramatic as in low-velocity dispersion groups, the cores of rich clusters are nonetheless very harsh environments for the fragile galaxian disks which pass through them. Not only is the density of galaxies much higher than in loose groups, but also cluster cores are often pervaded by a hot ($T \simeq 10^8$ K) intracluster medium responsible for the observed extended X-ray emission. A variety of mechanisms have been proposed which could sweep the interstellar gas from the disk of a spiral moving through the cluster: these include galaxy-galaxy collisions, tidal interactions, ram pressure sweeping by the intra-cluster medium, and evaporation.

Evidence that the circumstance of cluster residence affects galaxy evolution is offered by a variety of observations. The intracluster gas is believed to exert sufficient pressure to bend radio source jets into a variety of head-tail morphologies. Galaxies in clusters have been shown to be much less likely than are field galaxies to exhibit the optical emission lines associated with active star formation. The segregation of early-type galaxies into cluster cores, in contrast with the more widespread distribution of spirals throughout low-density regions, has led to speculation about the removal of gas from galaxies in clusters. Yet the bulk of the evidence, particularly concerning lenticulars, has led to the conclusion that much of the observed morphological segregation was introduced early in the galaxy formation era.

As a tracer of potential star formation, the neutral hydrogen content of galaxies serves as a probe of the efficiency of proposed gas removal mechanisms. In 1973, Davies and Lewis concluded that galaxies in the Virgo cluster possessed a lower HI surface density than did their counterparts in the field. Although that initial study was limited because of selection effects, particularly the Malmquist (luminosity) bias, its conclusions have been borne out by more recent observations. At present, data suitable for analyses of the comparative HI content of spirals now exist for more than ten clusters and for the field. The clusters studied generally contain a sizable population of spirals and are at redshifts less than $z = 0.04$. Some of the clusters have a high galaxian density, conducive to galaxy-galaxy interaction mechanisms, while others are characterized by high cluster X-ray luminosity, implying the presence of a healthy intracluster medium which is producing thermal bremsstrahlung emission. Thus, not only can we test the reality of the HI deficiency in cluster spirals, but also we can investigate the nature of the gas removal

process.

As the nearest rich cluster and center of the Local Supercluster, the Virgo cluster provides a laboratory for the investigation of environmental influences on the HI distribution and content of its member spirals. Virgo is dynamically still evolving. Its ellipticals and spirals form separate populations, and it appears that while the ellipticals form a relaxed, collapsed cluster core, the spirals are still infalling. The spirals in the Virgo core are large and near enough that the HI distribution can be mapped in some and the HI content can be measured in many. Numerous authors have carried out such observations of Virgo spirals using Arecibo, Naneay, Effelsberg, Westerbork, and the VLA and consistently find that spiral galaxies in the Virgo core are HI poor with respect to field galaxies. A substantial fraction of galaxies covering a wide range in luminosity and morphological type exhibit HI deficiency by factors which exceed ten. Furthermore, the Virgo core spirals have shrunken HI disks; in many, the HI disk is actually smaller than the optical extent. The latter observation, implying that the outer portions of the HI disk have been swept, is a forceful argument in support of external gas removal mechanisms. A number of Virgo spirals have now been mapped in the CO 2.6-mm line. CO emission traces the distribution of the dense molecular material in spiral disks. Kenney and Young (1986) find that the molecular disks, which are more centrally confined than the HI, show no trace of perturbation, reinforcing the finding based on HI data that sweeping affects primarily the outer gas layers.

The two Abell clusters A2151 and A2147 in the Hercules supercluster provide the opportunity to compare predictions of galaxy-galaxy interaction sweeping models with those of galaxy-intracluster gas ones. Lying at the same distance, the two clusters are quite different in their morphology. A2151 is a dehser, and yet more loosely organized, cluster and is associated with a relatively weak X-ray source, while A2147 appears azimuthally symmetric and exhibits a higher X-ray luminosity. The degree of HI deficiency is more pronounced in A2147. Further comparison of the HI deficiencies observed in nine clusters by Giovanelli and Haynes (1985a) shows that the degree of HI deficiency seen in a cluster correlates with the presence of a hot intracluster medium, as implied by cluster X-ray emission. The exact nature of the gas removal process, either ram pressure sweeping by the intracluster gas as the galaxy moves through the cluster, evaporation, or a more complicated combination of the two, is yet elusive. However, it seems that spiral disks which pass through the hostile cluster core lose as much as 90% of their initial HI mass but retain most of their denser molecular clouds. The HI-poor galaxies furthermore show evidence for reduced star formation rates; that is, they are redder than field galaxies of similar morphology. At comparable galaxian densities, the fraction of galaxies which are classified as lenticular is significantly higher, while that of spirals is correspondingly lower, in clusters with high-X-ray luminosity; this suggests that a causal relationship might exist between morphological type and current cluster conditions. While not all cluster S0's need be swept spirals, the observed HI deficiency in, cluster spirals does argue that some reinforcement of the initial morphological segregation occurs in environments hostile to diffuse interstellar gas.

12.7. COSMOLOGICAL STUDIES

Observations of 21-cm line radiation allow the exploration of cosmological questions because the

processes leading to either emission or absorption are generally well understood. The redshifts measured with commonly available HI line spectrometers are among the most accurate. While galaxies of high optical surface brightness dominate volumes of high galaxy density, the low-surface-brightness objects found in the regimes of groups and supercluster peripheries are usually HI rich and thus are easily studied by 21-cm techniques. Furthermore, since the HI signature of an HI disk is distinctive, the observation of the characteristic two-horned 21-cm profile can testify to the presence of a gas-rich disk structure even in objects not visible optically. The 21-cm line thus serves not only as the complement of observations made at other wavelengths but can, in some cases, provide information not obtainable any other way.

In this section, we discuss further the use of 21-cm line studies to address questions of cosmological relevance. The use of the velocity width-magnitude relation to measure deviations from the Hubble flow has already been discussed in Section 12.4.2. In conjunction with measures made at other wavelengths, 21-cm line observations are critical to our understanding of the structure and evolution of the universe.

12.7.1. 21-cm Redshift Surveys

In contrast with studies at optical wavelengths, HI redshift surveys are especially applicable to objects that cluster least and are therefore useful for studying the large-scale structure of the galaxy distribution. The spectacular surge of interest in the study of the large-scale structure of the universe that has occurred in the last decade has stimulated the undertaking of massive surveys to determine the radial velocities of galaxies at progressively fainter magnitude levels. While the emphasis at the beginning of the 1980s was mainly on the rough mapping and the determination of the scale of the inhomogeneities in the distribution of luminous matter, attention has more recently shifted to the topology of the galaxian distribution and its segregation properties. Entering an area traditionally the monopoly of optical instruments, large-aperture radio telescopes have become important as redshift machines. In this section, we will review the technical aspects of redshift surveys, and in the next one, some of their results will be presented.

Following Table 12.1, we can assume that the mean expectation value for the HI mass of a spiral galaxy is on the order of $3 \times 10^9 M\odot$ (for $h = l$, as will be assumed throughout this section). Via Equation (12.3), that mass translates into a flux integral of $1.3 \times 10^4 d^{-2}$ Jy km s^{-1}, where d is the distance to the galaxy in Mpc. For a most probable inclination of the disk, an observed velocity width of about 400 km s^{-1} should be expected; if we express the distance in terms of a radial velocity v_3 (in 1000 km s^{-1} units), the average flux density of the galaxy over the line profile will be $320 v_3^{-2}$ mJy. For comparison, a typical HI observation of 5 minutes on source plus 5 minutes off source (for subtraction of sky and instrumental effects) yields an rms noise of about 1 mJy, at 20-km s^{-1} resolution, with the Arecibo 305-m telescope (using a GaAs FET receiver and the current line feed system, which give a system temperature of 35 to 65 K, depending on the zenith distance of the source). Because the signal will be spread over many channels, an average signal-to-noise ratio of 2 will be more than sufficient to ensure detection. In other words, a "typical" spiral can be detected in one "on-off" pair, at Arecibo, out to a

distance corresponding to + 15,000 km s^{-1}. Such a radial velocity is larger than the characteristic redshift "depth" of most galaxy catalogues, such as the *Uppsala General Catalogue* (Nilson 1973) or the *Catalogue of Galaxies and Clusters of Galaxies* (Zwicky et al. 1961-68), which, combined, provide listings for about 30,000 galaxies in the northern hemisphere. Improvements in receiver technology and other instrumental upgrades promise to expand the number of accessible sources by one order of magnitude in the next few years.

Unlike continuum surveys with single-dish radio telescopes, 21-cm redshift surveys are not confusion limited. Adding the third dimension provided by the radial velocity guarantees that the vast majority of sources will be separable, even in high-density environments such as clusters. Confusion - or the inability to separate line blends - only occurs in very tight pairs or groups with small velocity dispersions and affects less than 1% of all surveyed sources.

Currently, other instrumental limitations, besides sensitivity, limit the scope of 21-cm redshift surveys. Standard autocorrelation spectrometers allow instantaneous coverage of velocity windows on the order of +8000 km s^{-1}. Thus, in spite of the fact that angular size is, to the first order, a good distance indicator, the search for the 21-cm line emission of a given galaxy may take several observations in contiguous velocity ranges. Currently, effective redshift searches of 21-cm emission are limited to velocities below + 25,000 km s^{-1}. Man-made interference constitutes a severe handicap at some frequencies of interest for the redshifted 21-cm line, and special precautions, such as lateral shielding of the receiving feed sytem or software excision of interfering signals, are becoming necessary.

The first extensive 21-cm survey of cosmological significance was conducted by Fisher and Tully (1981), on a sample of approximately 2000 galaxies in the Local Supercluster. Currently, a sample about twice as large is nearing completion in the Pisces-Perseus supercluster region (Giovanelli and Haynes 1985b), and somewhat smaller efforts are under way in the Cancer and Hercules regions (Bicay and Giovanelli 1986). Figure 12.9 displays partial results of the Pisces-Perseus survey, including the mapping of a long filamentary structure which probably extends well beyond the boundaries of the surveyed region. The Local Supercluster is also being studied to fainter levels, with current attention concentrating on the characteristics of the dwarf galaxy population (Hoffman et al. 1987).

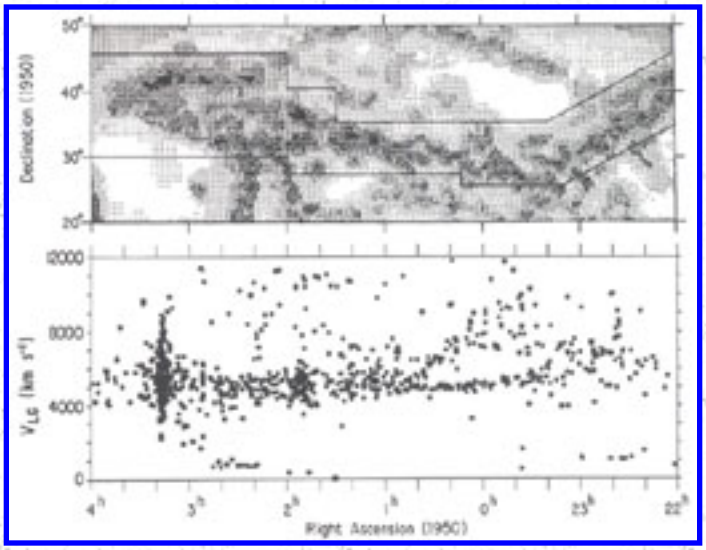

Figure 12.9. The upper panel displays the density of galaxies brighter than m = 15.7 per unit solid angle, as contours of different shade intensity. The lower panel illustrates the radial velocity distribution, as a function of Right Ascension, of the galaxies which are contained within the jagged contour outlined in the upper panel, emphasizing the existence of a three-dimensional structure which coincides with the enhancement in the surface density visible in the upper panel (From Giovanelli et al. 1986).

12.7.2. Voids and the Segregation of Galaxian Properties

Progress in the collection of radial velocity data, both by optical and radio means, has made clear that the distribution of optically luminous matter may be outlined by regions of enhanced density mixed with "voids," regions largely evacuated of luminous matter. Density contrasts on the order of 10 to 100, between the large-scale high- and low-density regions, are common. Currently popular cosmological models require the universe to have a mean density equal to the critical value (i.e., one that will asymptotically reduce the expansion rate of the universe to zero). The majority of matter necessary to achieve critical density is not visible and probably not in baryonic form. Virial analysis of groups and clusters of galaxies indicates that if the universe has indeed the critical density, the dark matter is not as clumped as are the luminous galaxies. It then appears difficult to understand how the baryonic component - in this scheme, a dynamically minor component of the universe - would have separately evolved to the high degree of clustering that is observed. One possible solution to the problem is that the baryonic mass distribution, in spite of the highly contrasted picture offered by the bright galaxies, is actually only slightly nonhomogeneous. In that case, one must postulate that galaxy formation is a threshold process. If bright galaxies only formed in 2- to 3σ peaks of the density fluctuations of pregalactic material, bright galaxy formation thrived in regions dominated by large-scale perturbations

slightly above the average density. That process was inhibited, however, in large-scale regions with mean density slightly below the universal average. This scheme would result in a large apparent amplification of the density contrast; such "biasing" of the galaxy formation process is well described by Rees (1985).

We may then address the observational questions of whether "voids" are actually devoid of baryonic matter or are populated by less conspicuous conglomerates such as very-low-luminosity galaxies. The answers require the study of samples of intrinsically faint galaxies over large volumes. Because' their surface brightness is also low, such objects become increasingly difficult targets of optical surveys. A large number of them are HI rich, however, because a large fraction of their mash is in the form of HI (See Section 12.5).

Recent studies (Bothun et al. 1986, Oemler 1986) indicate that dwarf galaxies are far from filling the voids. Studies of larger samples (such as that in the Pisces-Perseus supercluster, mentioned in Section 12.7.1) suggest that the density contrast between low- and high-density regions diminishes with the intrinsic luminosity of the galaxian population. This effect is sketched in Figure 12.10, where the density contrast within a large solid angle encompassing a conspicuous void in the Pisces-Perseus supercluster region is illustrated separately for bright and faint galaxies. The relative excess or deficiency of galaxies is estimated in comparison with the expectation from a skywide determination of the galaxian luminosity function. It shows that the density contrast between high- and low-density regions diminishes for fainter galaxies, a trend in the direction indicated by biased galaxy formation schemes.

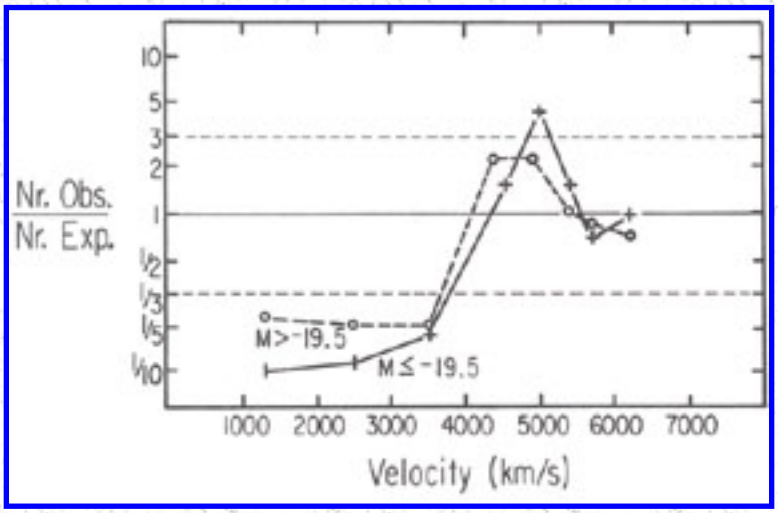

Figure 12.10. The ratio between the number of galaxies observed and the number which would be expected from a homogeneously distributed population, plotted as a function of radial velocity within a solid angle which encloses both a foreground "void" and part of the high-density enhancement seen in Figure 12.9 near 5000 km s^{-1}. The ratio is plotted separately for bright and fainter galaxies (the label of each curve corresponding to a photographic absolute magnitude limit). Notice that both the depression associated with the void and the peak associated with the supercluster are milder when seen with a "filter" which excludes the brightest galaxies.

The effect illustrated in Figure 12.10 indicates that there is luminosity segregation between different local density regimes. Other forms of segregation according to morphological type, gas content, and total mass are present. Such variations are intimately related to the physical processes that led to galaxy formation. Some of these effects, such as the local density dependence of the gas content, can be exacerbated in particularly active environments, such as the cores of clusters, as was described in Section 12.6. Those secularly occurring effects, however, may be small-scale alterations to the inbred characteristics of the galaxian population.

As an alternative component of baryonic matter capable of making a contribution to the mass density distribution, the existence of not fully collapsed intergalactic clouds of HI has been postulated. Searches, both directed and serendipitous, for such objects (Krumm and Brosch 1984, Altschuler et al. 1987) have been unsuccessful. Whether diffuse HI is abundant in intergalactic space is, however, a relatively open question because the dominating excitation process of the hyperfine levels and the spectral signature of possible HI features are still largely uncertain.

An alternative mode of investigating the dynamic mass contrast, i.e., whether the overall mass distribution is traced by that of luminous galaxies, consists in studying the magnitude of large-scale peculiar motions of galaxies. If voids are indeed devoid of mass, then substantial deviations from a smooth Hubble flow, as discussed in Section 12.4.2, should be visible in the population of galaxies near their edges.

12.7.3. HI in Active Galaxies

Some of the most luminous galaxies in the universe are those that are undergoing an enhanced phase of activity. The term "active" is applied to galaxies that are undergoing a variety of processes that increase the total luminosity of the host galaxy. Most often, the activity is confined to the nucleus or the inner

few kiloparsecs of the galaxy. Seyfert galaxies contain bright, starlike nuclei and exhibit broad emission lines. The survey performed by the Infrared Astronomical Satellite (IRAS) in the wavelength range from 10 to 100 ym has revealed a new category of objects that are ultraluminous in the far-infrared. bands. More often than not, these objects show signs of interaction with companions; and their enhanced infrared luminosity results from the heating of dust by ultraviolet photons emitted in a burst of star formation [see the review by Soifer et al. (1987)]. Even the Milky Way harbors energetic phenomena in its own nucleus,'and it is likely that many galaxies will be active for some portion of their lifetime.

The Seyfert phenomenon occurs most often in early-type spirals and is proposed to result from the powering of nuclear activity by the accretion of gas onto a massive object in the center of the galaxy (Weedman 1986). HI surveys of Seyfert galaxies as have been conducted by Heckman et al. (1978) and Mirabel and Wilson (1984) help to establish the nature of the galaxy containing the Seyfert nucleus. While for the majority of Seyfert galaxies, the ratio of hydrogen mass to optical luminosity, M_H / L, is similar to that expected for galaxies of similar optical morphology, some Seyferts appear to be usually gas rich. The redshifts obtained from the 21-cm line observations are systematically larger than those derived from the nuclear optical emission lines, suggesting a net outflow of gas in the narrow-emission line regions. A significant percentage, 40% or so, of detected Seyfert galaxies show highly asymmetric HI profiles, not the characteristic two-homed ones expected from quiescent spiral disks. It is not yet known whether these deviations arise from interactions with companions, ionization of significant HI in selected regions of the disk, or blending of more than one emitting galaxy within the single-dish beam.

Because active galactic nuclei are often the hosts of compact radio continuum sources, 21-cm absorption as well as emission may often be seen both in Seyfert galaxies and in others that are radio sources. As illustrated in Equation (12.1), an HI cloud of total optical depth τ which is bathed in a radiation field with a significant flux at 21-cm wavelength will produce a spectrum that is the combination of the emission by (and self-absorption within) the cloud and the absorption of the continuum radiation originating behind the absorbing cloud. Because of the magnetic dipole nature of the 21-cm line transition, and of the fact that a significant correction of stimulated emission must be applied to τ, the 21-cm line optical depth is normally very low. Because of this small opacity, the detection of HI in absorption is possible only where the line of sight to a source of radio continuum emission passes through an HI region with a large column density, N_H, of neutral hydrogen. The resulting opacity τ is determined by the ratio N_H / T_s, where T_s is the spin temperature, as described in Section 12.1.2. If NH can be derived from measurements at other spectral regimes, τ can then provide an estimate of the excitation characteristics of the gas. Furthermore, the ability of a source to appear in absorption, given some value of optical depth for the intervening HI region, depends only on its continuum flux density, not on its distance. Thus, HI absorption can be detected in objects at very high redshift; such objects need not be particularly massive in HI, but only optically thick along the line of sight and favorably positioned in front of a relatively strong continuum source.

Obviously, absorption lines are produced against sources which emit strongly in the radio continuum, and so information is gleaned only about the line of sight to such sources. HI absorption has been detected in some two dozen galaxies, with typical optical depths of a few hundredths found. Most

typically, absorption is seen against a continuum source which is located in the galaxy's center. Absorption arises in clouds contained in the same galaxy, perhaps in its disk. Optical depths are derived on the assumption that the absorbing cloud (or clouds) covers the continuum source completely. If the cloud actually covers only a portion of the illuminating source, the optical depths will be underestimated.

In fact, only a small fraction of radio galaxies, including spirals and ellipticals with prominent dust lanes, exhibit HI absorption. Figure 12.11 shows the HI emission and absorption observed in the lenticular galaxy NGC 1052; the absorption profile is obtained in the direction of its central continuum source. The geometry of the source relative to potential absorbers plays a critical role. While narrow HI absorption features are seen in many active galaxies, those observed in others are broad and resemble features seen in lines of the OH radical. The HI absorption is often found offset from the galaxian systemic velocity, as would be expected if the absorbing material is infalling into the nuclear region. However, exceptions do occur; several cases of HI absorption show features that are blue-shifted by 100 km s^{-1} or more with respect to the galaxy's line emission centroid (Dickey 1982). Detailed maps of the absorption and (when detectable) emission are required in order to establish the location and kinematics of the gas.

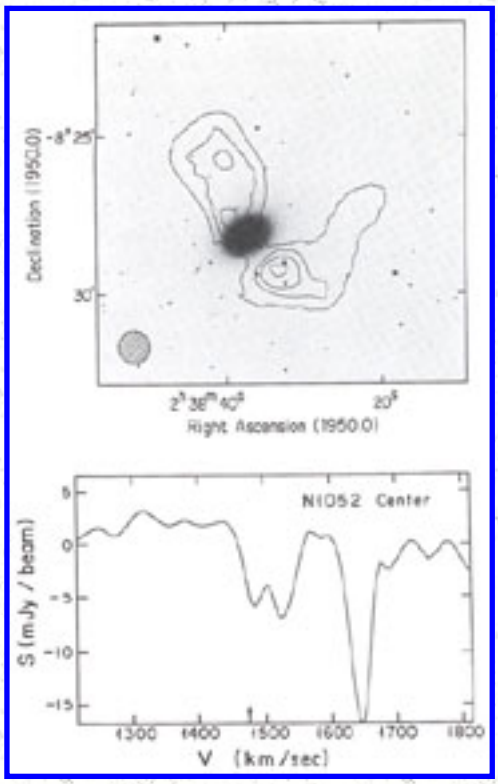

Figure 12.11. *Top:* HI distribution in the early-type galaxy NGC 1052, obtained with the very Large Array by van Gorkom et al. (1986). Contours correspond to HI column densities of 0.15, 0.6, 1.07 and 1.83 × 10^{20} cm^{-2}. *Bottom:* absorption profile obtained against the galaxy's nuclear continuum source.

The far-infrared emission detected by IRAS arises from both normal and peculiar galaxies. The dominant population of galaxies that are bright in the far infrared are spirals. The infrared emission is likely to arise from two dust components in the disk: a component closely associated with star formation activity in HII regions and molecular cloud complexes, and a second that is heated by the diffuse inter-stellar radiation field. The latter is identified with the so-called "infrared cirrus" seen in the Milky Way. The exact correlation of these two components with HI in our own galaxy and external galaxies is still under investigation.

Some of the galaxies that are overluminous in the far infrared and particularly identified to have very high star formation rates earn the designation of "starburst" galaxies. The high occurrence of multiplicity and peculiar morphology in these systems suggests that the current burst of star formation is somehow triggered by the interaction process between close companions. Observations of atomic hydrogen in such systems identify them as spirals because their hydrogen masses are generally large, typical of spirals but not earlier-type systems. In a significant fraction, the shape of the HI profile indicates the presence of global disturbances. In the most peculiar of these systems, such as the merger candidate Arp 220, there is a striking absence of atomic gas in locations where molecular hydrogen is found, indicating an enhancement of the atomic-to-molecular conversion process that must ultimately then lead to a higher star formation rate.

Low-optical-luminosity blue compact dwarf (BCD) galaxies, sometimes referred to as "extragalactic HII regions," also seem to be undergoing active star formation. Like the blue star light, the HI emission is patchy and the HI clumps actually avoid the brightest optical features. Like the normal dI's, the HI usually extends well, beyond the optical image. It is not at all clear what triggers star formation in some dwarfs and not in others, even though the HI column densities in both types may remain in excess of N_H = 10^{20} cm^{-2} even beyond the optical radius.

12.7.4. HI in Quasars and in Their Spectra

The host galaxies of quasars (QSOs) are difficult to observe at most wavelengths because the line and continuum radiation from the underlying galaxy is usually overwhelmed by the central QSO itself. And, although the optical galactic envelopes of QSOs have been observed to a redshift of about 0.5, these envelopes are sufficiently small over such distances that it is difficult to choose whether they are better

fit by a spheroidal $r^{1/4}$ law or by an exponential disk. The optical "fuzz" surrounding the nearest QSOs does seem to be fainter than expected for typical luminous ellipticals and sometimes suggests a spiral, though deformed, morphology. Just as the characteristic two-horned 21-cm profile can be used to place Seyfert and starburst galaxies in the heart of an otherwise faint or even unseen spiral disk, the detection of 21-cm emission from QSOs can be used as further evidence that the host object is likely a spiral (Condon et al. 1985). The detection of HI indicates the presence of gas in the host. Symmetric HI profiles can be used to determine an accurate systemic redshift that can be compared with the optical emission line values to establish the kinematics and radiation transfer within the regions producing. the narrow and broad optical lines. Asymmetric 21-cm line profiles may indicate the presence of tidal disruption or other global disturbances that may contribute to the QSO activity or result from it. Several QSOs are now known to reside in galaxies containing on the order of 7×10^9 $M_\odot$ of HI, a typical HI mass for a spiral galaxy but much larger than that expected for an elliptical.

The optical spectra of QSOs frequently contain very narrow absorption lines nearly always lying at lower redshift z_{abs} than the emission redshift z_{em}, itself derived from the broad high-excitation emission lines also present. The location of the absorbing clouds has always been controversial: do they lie close to the quasar itself and move away from the quasar with relativistic velocities or are they located at some intermediate distance, corresponding to a strict cosmological recession-velocity interpretation of z_{abs} ?

Under the assumption that clouds producing the narrow absorption lines are cold, the spectra of many quasars which are radio continuum sources have been searched for redshifted 21-cm absorption. Detectable absorption is expected if a cloud of $N_H > 1.0 \times 10^{20}$ cm^{-2} and $T_s < 1000$ K intercepts the line of sight. Such clouds are prevalent in the disk of the Milky Way. Searches are made difficult by bandwidth and spectral resolution restrictions of current instrumentation, which limits the instantaneous frequency search range to a few tens of MHz, and by the presence of man-made interference - an increasingly severe handicap - at frequencies below 1 GHz. Nevertheless, absorption of redshifted HI has been detected in about ten QSOs.

The first detection of the 21-cm line in a quasar spectrum was made by Brown and Roberts (1973), who detected it in absorption at 839 MHz in 3C286, corresponding to a redshift of $z_{abs} = 0.69$. The half-width of the line in the rest frame was observed to be 8.2 km s^{-1}. VLBI observations reveal the existence of two narrow-velocity features of dispersion 1.6 and 3.0 km s^{-1}, each located in front of a compact component in the continuum source. The inferred column densities are high, in excess of $8.5 \times 10^{19}(T_s /$ 100 K) cm^{-2}, reminiscent of those seen in the disk of the Milky Way. After the discovery of the absorption at 21 cm, weak absorption features identified with transitions in MgI, MgII, and FeII were detected at optical wavelengths. In Milky Way clouds, the element Mg appears mainly in its singly ionized form; therefore, it appears sensible to search for MgII and HI arising from the same absorber. In such a search, Briggs and Wolfe (1983) found only two coincidences among eighteen redshifted clouds searched; most optical redshift systems do not contain highly opaque HI gas. Briggs and Woffe concluded that there is no correlation between 21-cm optical depth and such optical properties as MgII equivalent width, MgII doublet ratio, or MgI equivalent width. This lack of correlation between the

radio and optical properties can be explained if the opacity is only occasionally high enough to produce HI absorption, and even in those cases, the HI clouds do not contribute significantly to the optical equivalent widths. Two gas phases are inferred: one showing only optical absorption, similar to Milky Way halo clouds, and one showing also 21-cm absorption characteristic of clouds in a galaxian disk similar to our own.

Perhaps the most intriguing 21-cm absorption line system is the one exhibited by the BL Lac object AO 0235+164, discovered by Roberts et al. (1976). This system is the first in which both radio and optical high-redshift absorption lines were measured at coincident redshifts. Figure 12.12 shows the $z_{abs} = 0.52$ line, which occurs at 932 MHz. This spectrum, observed with a resolution of 1.6 km s^{-1}, reveals five separate HI clouds in front of the source. Two gas phases are required to explain both the distinct narrow features and the overall absorption. The narrow features represent high-column-density clouds, each characterized by a velocity dispersion of about 3 km s^{-1} spread over a-range in mean velocity of 105 km s^{-1}. In order to fit adequately the optical curve of growth, however, an additional component, optically thin at 21 cm and having a velocity dispersion of about 40 km s^{-1}, must also be present.

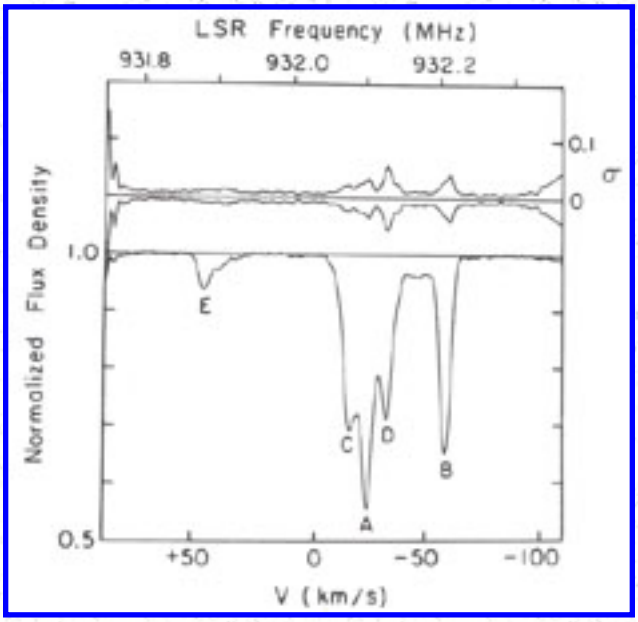

Figure 12.12. HI absorption line against the BL Lac object AO 0235+164, obtained with the Arecibo telescope by Wolfe et al. (1982).

If intervening galaxian disks are to be invoked to explain absorption lines in the spectra of quasars, the extrapolation to high redshift of a "normal" luminosity function and of commonly observed sizes of gaseous disks at low redshift cannot explain the observed number of absorption features. A different population of objects from those seen at low redshift or spiral disks that are much larger than their present-day counterparts appear to be necessary. Models of galaxy evolution that have been constructed to explain both the present metallicity and stellar luminosity function predict that in its early history, the typical column density of HI in the disk of the Milky Way was three to ten times higher than it is today;

the velocity dispersion in the gas might have been as much as ten times larger than the current value of 10 km s^{-1}. It is not yet clear whether galaxy disks existed at a redshift of 2 or more, or alternatively whether the growth of disks-was a slow process taking more than 10^{10} years after collapse to reach the Holmberg radius. As this field of research is still in a highly speculative stage, the 21-cm line appears to be a most promising probe of the universe at high redshifts.

This chapter was initially compiled in mid-1985 and revised in March 1987. The authors wish to thank M.S. Roberts, R. Sancisi and the editors for careful reading and useful suggestions on earlier versions of the manuscript.

Recommended Reading

- Roberts, M.S. 1975. In A. Sandage, M. Sandage and J. Kristian (eds.), Galaxies and the Universe. Chicago: University of Chicago Press, p. 309.

- Sancisi, R. 1981. In S.M. Fall and D. Lynden-Bell (eds.), The Structure and Evolution of Normal Galaxies. Cambridge: University Cambridge Press, p. 149.

- Haynes, M.P., R. Giovanelli, and G.L. Chincarini. 1984. Annual Rev. Astron. Astrophys. 22:445.

REFERENCES

1. Aaronson, M., J. Huchra, and J. Mould. 1979. Astrophys. J. 229:1.
2. Aaronson, M., J. Huchra, J.R. Mould, R.B. Tully, J.R. Fisher, H. van Woerden, W.M. Goss, P. Chamaraux, U. Mebold, B. Siegman, G. Berriman, and S.E. Persson. 1982. Astrophys. J. Suppl. Ser. 50:241.
3. Aaronson, M., G. Bothun, J. Mould, R.A. Schommer, and M.E. Cornell. 1986. Astrophys. J. 302:536.
4. Altschuler, DA., M.M. Davis, and C. Giovanardi. 1987.Astron. Astrophys. 178:16.
5. Bicay, M.D., and R. Giovanelli. 1986. Astron. J. 91:732.
6. Bosma, A. 1981a. Astron. J. 86:1791.
7. Bosma, A. 1981b. Astron. J. 86:1825.
8. Bothun, G.D., T.C. Beers, J.R. Mould, and J.P. Huchra. 1986. Astrophys. J. 308:510.
9. Bottinelli, L., L. Gouguenheim, G. Paturel, and P. Teerikorpi. 1986, Astron. Astrophys: 156:157.
10. Brinks, E., and E. Bajaja. 1986. Astron. Astrophys. 169:14.
11. Brinks, E., and W.W. Shane. 1984. Astron. Astrophys. Suppl. Ser. 55:179.
12. Briggs, F.H., and A.M. Wolfe. 1983. Astrophys. J. 268:76.
13. Brosche, P. 1971. Astron. Astrophys. 31:205.
14. Brown, R.L., and M.S. Roberts. 1973. Astrophys. J. (Lett.) 184:L7.
15. Burstein, D. 1982. Astrophys. J. 253:539.

16. Carignan, C., R. Sancisi, and T.S. van Albada. 1987. Astron. J. (to be published).
17. Condon, J.J., J.B. Hutchings, and A.C. Gower. 1985. Astron. J. 90:1642.
18. Cottrell, GA. 1978. Mon. Not. R. Astron. Soc. 184:259.
19. Davies, R.D., and B.M. Lewis. 1973. Mon. Not. R Astron. Soc. 165:231.
20. Dickey, J.D. 1982. Astrophys. J. 293:87.
21. Ewen, H.I., and E.M. Purcell. 1951. Nature 168:356.
22. Faber, S. 1982. In HA. Bruck, G.V. Coyne, and M.S. Longair (eds.), Astrophysical Cosmology. Citta' del Vaticano: Pont. Acad. Scient., p. 191.
23. Field, G.B. 1959. Astrophys. J. 129:536.
24. Fisher, JR., and R.B. Tully. 1975. Astron: Astrophys. 44:151.
25. Fisher, J.R., and R.B. Tully. 1981. Astrophys. J. Suppl. Ser. 47:139.
26. Giovanelli, R, and M.P. Haynes. 1985x. Astrophys. J. 292:404.
27. Giovanelli, R., and M.P. Haynes. 1985b. Astron. J. 90:2445.
28. Giovanelli, R., M.P. Haynes, and G.L. Chincarini. 1986. Astrophys. J. 300:77.
29. Hart, L., and R.D. Davies. 1982. Nature 297:191.
30. Haynes, M.P., and R. Giovanelli. 1984. Astron. J. 89:758.
31. Haynes, M.P., R. Giovanelli, and M.S. Roberts. 1979. Astrophys. J. 229:83.
32. Haynes, M.P., R. Giovanelli, and G.L. Chincarini. 1984. Annu. Rev. Astron. Astrophys. 22:445.
33. Heckman, T.M., B. Balick, and W.T. Sullivan III. 1978. Astrophys. J..224:745.
34. Hoffman, L.G., G. Helou, E.E. Salpeter, J. Glosson, and A. Sandage. 1987. Astrophys. J. Suppl. Ser, 63:247.
35. Huchtmeier, W.K., J. Seiradakis, and J. Materne. 1981. Astron. Astrophys. 102:134.
36. Johnson, D., and S. Gottesman. 1983. Astrophys. J. 275:549.
37. Jura, M., D.W. Kim, G.R. Knapp, and P. Guhathakurta. 1987. Astrophys. J. (Lett.) 312: Ll1.
38. Kenney, J., and J. Young. 1986. Astrophys. J. 301:L13.
39. Kerr, F.J., and J.V. Hindman. 1953. Astron. J. 56:218.
40. Knapp, G.R., E.L. Turner, and P.E. Cunniffe. 1985x, Astron: J. 90:454.
41. Knapp, G.L., W. van Driel, and H. van Woerden. 1985b, Astron. Astrophys. 142:1.
42. Krumm, N., and N. Brosch. 1984. Astron. J. 89:1461.
43. Lake, G., R.A. Schommer, and J. van Gorkom. 1987. Astrophys. J. 314:57.
44. Mirabel, I.F., and A.S. Wilson. 1984. Astrophys. J. 277:92.
45. Nilson, P. 1973. Uppsala General Catalogue of Galaxies. Uppsala Astron: Obs. Ann. 6.
46. Oemler, A. 1986. In S.M. Faber (ed.), Nearly Normal Galaxies: From the Planck Time to the Present Time. New York: Springer-Verlag, p. 213.
47. Rees, M.J. 1985. Mon. Not. R. Astron. Soc. 213:75P.
48. Richter, O.-G., W.K. Huchtmeier, H.-D. Bohnenstengel and M. Hausschildt. 1983. ESO preprint nr. 250.
49. Roberts, M.S. 1975. In A. Sandage, M. Sandage, and 1. Kristian (eds.), Galaxies and the Universe. Chicago: University of Chicago Press; p. 309.
50. Roberts, M.S. 1978. Astron. J. 83:1026.
51. Roberts, M.S., R.L. Brown, W.D. Brundage, A.H. Rots, M.P. Haynes, and A.M. Wolfe. 1976. Astron. J. 81:293.
52. Rots, A.H., and W.W. Shane. 1975. Astron. Astrophys. 45:25.

53. Rubin, V.C., D. Burstein, W.K. Ford, Jr., and N. Thonnard. 1985. Astrophys. J. 289:81.
54. Sancisi, R. 1976. Astron. Astrophys. 53:159.
55. Sancisi, R. 1981. In S.M. Fall and D. Lynden-Bell (eds.), The Structure and Evolution of Normal Galaxies. Cambridge: Cambridge University Press, p. 149.
56. Sancisi, R. 1983. In E. Athanassoula (ed.), Internal Kinematics and Dynamics of Galaxies, Int. Astron. Union Symp. 100. Dordrecht: Reidel, p. 55.
57. Sanders, R.H. 1980. Astrophys. J. 242:931:
58. Sargent, W.L.W., and K.-Y. Lo. 1986. In D. Kunth, T.X. Thann, and J. Tran Thanh Van (eds.), Star-Forming Dwarf Galaxies and Related Objects. Gif-sur-Yvette: Editions Frontiéres, p. 253.
59. Schneider, S.E., G. Helou, E.E. Salpeter, and Y. Terzian. 1986. Astron. J. 91:13.
60. Schweizer, F., B.C. Whitmore and V.C. Rubin. 1983. Astron. J. 88:909.
61. Shostak, G.S., W.T. Sullivan III, and R.J. Allen. 1984. Astron: Astrophys. 139: L5.
62. Soifer, B.T., J.R. Houck, and G. Neugebauer. 1987. Annu. Rev. Astron. Astrophys. (to be published).
63. Spitzer, L. 1978. Physical Processes in the Interstellar Medium. New York: John Wiley and Sons.
64. Toomre, A. 1983. In E. Athanassoula (ed.), Internal Kinematics and Dynamics of Galaxies, Int. Astron. Union Symp. 100. Dordrecht: Reidel, p. 177.
65. Toomre, J., and J. Toomre. 1972. Astrophys. J. 178:623.
66. Tully, R.B., and J.R. Fisher. 1977. Astron. Astrophys. 54:661.
67. van der Kruit, P.C., and G.S. Shostak. 1983. In E. Athanassoula (ed.), Internal Kinematics and Dynamics of Galaxies, Int. Astron. Union Symp. 100. Dordrecht: Reidel, p. 69.
68. van Gorkom, J., G.R. Knapp, E. Raimond, S.M. Faber, and J.S. Gallagher. 1986. Astron. J. 91-:791.
69. van Gorkom, J., P. Schechter, and J. Kristian. 1987. preprint.
70. van Woerden, H., W. van Driel, and U.J. Schwartz. 1983. In E. Athanassoula (ed.), Internal Kinematics and Dynamics of Galaxies, Int. Astron. Union Symp. 100. Dordrecht: Reidel, p. 99.
71. Wardle, M., and G.R. Knapp. 1986. Astron. J. 91:23.
72. Watson, W.D., and S. Deguchi. 1984. Astrophys. J. (Lett.) 281: L5.
73. Weedman, D. 1986. Quasar Astronomy. Cambridge: Cambridge University Press.
74. Wolfe, A.M., M.M. Davis, and F.H. Briggs. 1982. Astrophys. J. 259:495.
75. Zwicky, F., E. Herzog, M. Karpowicz, C.T. Kowal, and P. Wild. 1961-68. Catalogue of Galaxies and Clusters of Galaxies, 6 vols. Pasadena: California Institute of Technology Press.